Supporting Information

for

Donor-Functionalized Aza-Benzannulated Perylenediimides-based Ternary Blend Efficient Inverted Organic Solar Cells

Mohd Wazid[1$], Tarun[2$], Upendra Kumar Pandey[2*] and Rajneesh Misra[1*]

[1]Department of Chemistry, Indian Institute of Technology Indore,

453552 (India)

[2]Organic & Flexible Electronics Laboratory, Department of Electrical Engineering, Shiv Nadar Institution of Eminence, G.B. Nagar, Uttar Pradesh- 201314 (India)

[$] Equal Contribution

Methods and materials

All the moisture and oxygen-sensitive reactions were performed in an inert atmosphere using the standard inert atmosphere method. ^{1}H NMR spectra were measured on a Bruker Advance (III) 400 MHz/500 MHz, and $^{13}C\{^{1}H\}$ NMR spectra were measured at 100 MHz/125 MHz using $CDCl_3$ as the internal solvent. The 1H NMR chemical shifts are recorded in parts per

million (ppm) relative to the solvent residual peak ($CDCl_3$, 7.26 ppm). The $^{13}C\{^1H\}$ NMR shifts are reported relative to the solvent residual peak ($CDCl_3$, 77.16 ppm). The multiplicities are given as s (singlet), d (doublet), t (triplet), q (quartet), and m (multiple), and the coupling constant values (J) are reported in Hz. The UV-visible absorption spectra of all compounds were recorded in a PerkinElmer LAMBDA 35 UV-visible Spectrophotometer in DCM solvent at room temperature. Cyclic voltammograms (CVs) and differential pulse voltammetry (DPVs) were recorded on a PalmSens 4 electrochemical analyzer using glassy carbon as a working electrode, Pt wire as the counter electrode, and Ag/AgCl as the reference electrode. The scan rate was 50 mV s^{-1} for cyclic voltammetry. A solution of $(TBA)ClO_4$ in CH_2Cl_2 (0.1 M) was used as the supporting electrolyte. Molybdenum IV oxide, Zinc acetate di hydrate, 2-mehtoxy ethanol, ethanolamine, acetone, IPA, chloroform and Hellmanex solution were purchased from sigma Aldrich. The donor material Polymer D18 (PCE 18)[(2,6-(4,8-bis(5-(2-ethylhexyl-3-fluoro)thio phen-2-yl)-benzo[1,2-b:4,5-b']dithiophene)) alt-5,5'-(5,8-bis(4-(2-butyloctyl)thiophen-2-yl) dithieno[3',2':3,4;2'',3'':5,6]benzo[1,2c][1, 2, 5] thiadiazole)] **,** acceptor material NFAs Y6 (2,2'-((2Z,2'Z)-((12,13-bis(2 ethylhexyl)-3,9-diundecyl-12,13-dihydro-[1,2,5] thiadiazolo[3,4-e]thieno[2",3'':4',5']thieno[2',3':4,5] pyrrolo[3,2-g] thieno [2',3':4,5] thieno[3,2-b]indole 2,10-diyl)bis(methanylylidene)) bis(5,6-difluoro 3-oxo-2,3-dihydro-1H-indene-2,1-diylidene)) dima lononitrile), N,N'-Bis{3-[3-(Dimethylamino)propylamino]propyl}perylene-3,4,9,10-tetracarboxylic diimide (PDINN) were purchased from 1-Materials Company, Canada. Fluorene-doped tin oxide (FTO) (15–25 Ω/sq) was obtained from sigma.

Device fabrication details:

The inverted structure of OSCs fabricated with FTO/ZnO/**Active layer**/MoO_3/Ag configuration. The fabrication process began with etching the patterned FTO-coated glass by spreading zinc dust (Qualigens) and applying 2 M HCl solution in DI water for 2 minutes. Then

samples were cleaned systematically by hand rinsing with soap solution and rinsed with DI water then sonicated in Hellamanex solution (2% *v/v* solution in deionized water), in DI water, acetone, and IPA, 20 min for each step. Then samples were blow dried with nitrogen gas. The blow-dried samples were annealed at 70 ˚C for 20 mins and instantly treated with UV Ozone for 20 mins at the same temperature. The ETL layer of ZnO deposited with spin coating the solution at 4000 rpm for 60 sec and annealed at 180 ˚C for 1 hr. The ETL coated samples were transferred inside a nitrogen filled glovebox (Purchased from VEC solution India) with oxygen level below 1000 ppm and H_2 level below 0.5 ppm. The active materials (solution stirred overnight at RT) with 11 mg/mL in chloroform D/A ratio of 1:1.6 spin-coated dynamically at 2500 rpm for 30 s on ZnO coated substrates. Then annealed at 60 ˚C for 5 mins to remove the solvent. To deposit the electrodes samples were transferred to thermal evaporator (Purchased from HINDHIVAC, HHV). A 10 nm layer of molybdenum (VI) oxide (MoO_3) followed by a 100 nm silver was deposited using a metal mask under a vacuum pressure of approximately 6 × 10^{-6} bar. The active area of each device was 6 mm². Then *J-V* characteristics of the samples were measured using Keithley source meter 2450 (Tektronix company) under 1 Sun illumination using a solar simulator of class AAA (Sciencetech Solar Canada).

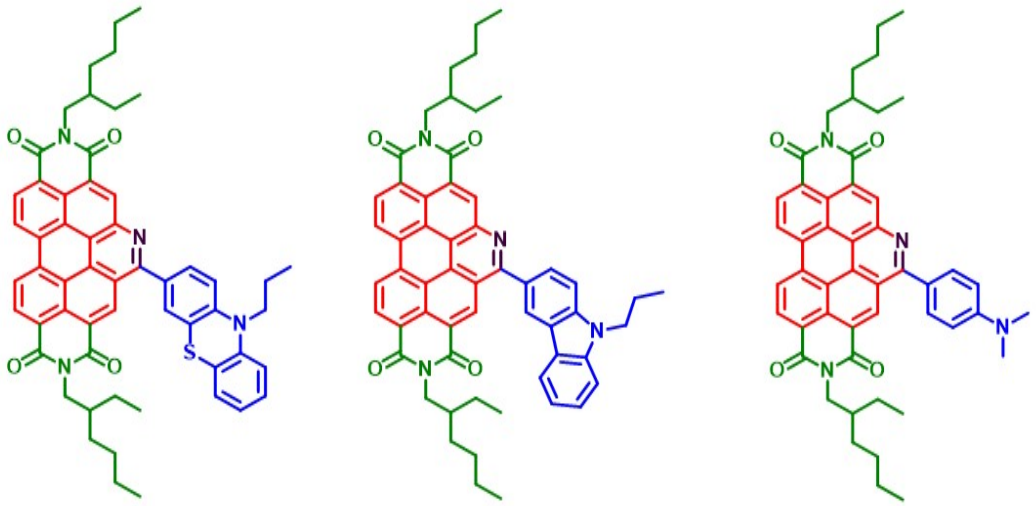

Figure S1: Molecular structure of **PTZPBI**, **CBZPBI,** and **NNDPBI** material

The lab-synthesized PBI's series materials (**PTZPBI**, **CBZPBI**, and **NNDPBI**) (molecular structure given in Figure S1) were incorporated with D18:Y6 in ternary OSCs. The detailed description regarding **CBZPBI** incorporated ternary devices (**D18:Y6: CBZPBI**) is given in main text. The **PTZPBI** and **NNDPBI** in ternary OSCs with active layer **D18:Y6: PTZPBI** and **D18:Y6: NNDPBI** respectively introduced by replacing the 20% of Y6 with same amount of **PTZPBI** and **NNDPBI**. This weight ratio of 20% is chosen based on the best results of ternary device with **CBZPBI** compound. Figure S2 d representing the power conversion efficiency (PCE) of ternary organic solar cells with all three PBI's acceptor material (20% weight ratio in replacement to Y6) with base D18:Y6 devices. Figure S2, also representing the carrier mobility and optical absorption of **PTZPBI** and **NNDPBI** acceptor materials.

Table S1: PCE data of D18:Y6 and ternary device with 20% of **PTZPBI**, **CBZPBI**, and **NNDPBI**, respectively.

Device	**Percentage of PBI's** ***(w/w)***	**J_{SC}** ***(mA/cm²)***	**V_{OC}** ***(Volt)***	**Fill Factor (*FF*)**	**Efficiency (*η*)**
D18:Y6	0%	24.28 ± 0.46	0.82 ± 0.005	0.69 ± 0.01	13.96 ± 0.17 %
D18: PTZPBI: Y6	20%	21.30 ± 0.69	0.81 ± 0.011	0.56 ± 0.04	09.89 ± 0.79 %
D18: CBZPBI: Y6	20%	24.39 ± 0.43	0.84 ± 0.003	0.72 ± 0.01	14.85 ± 0.18 %
D18: NNDPBI: Y6	20%	22.00 ± 1.00	0.83 ± 0.006	0.64 ± 0.01	11.71 ± 0.53%

However instead of showing good electron mobility and absorption outside of D18 and Y6 absorption range for both **PTZPBI** and **NNDPBI** compounds, their incorporation in ternary devices didn't show any improvements in PCE compared to the base devices, data given in Table S1. The average performance with **PTZPBI** and **NNDPBI** was due to improper energy alignment with D18 polymer donor and Y6 non-fullerene acceptor material, this non-ohmic

contact formation hinders the efficient transfer of carriers to the respective electrodes as represented in Figure S3.

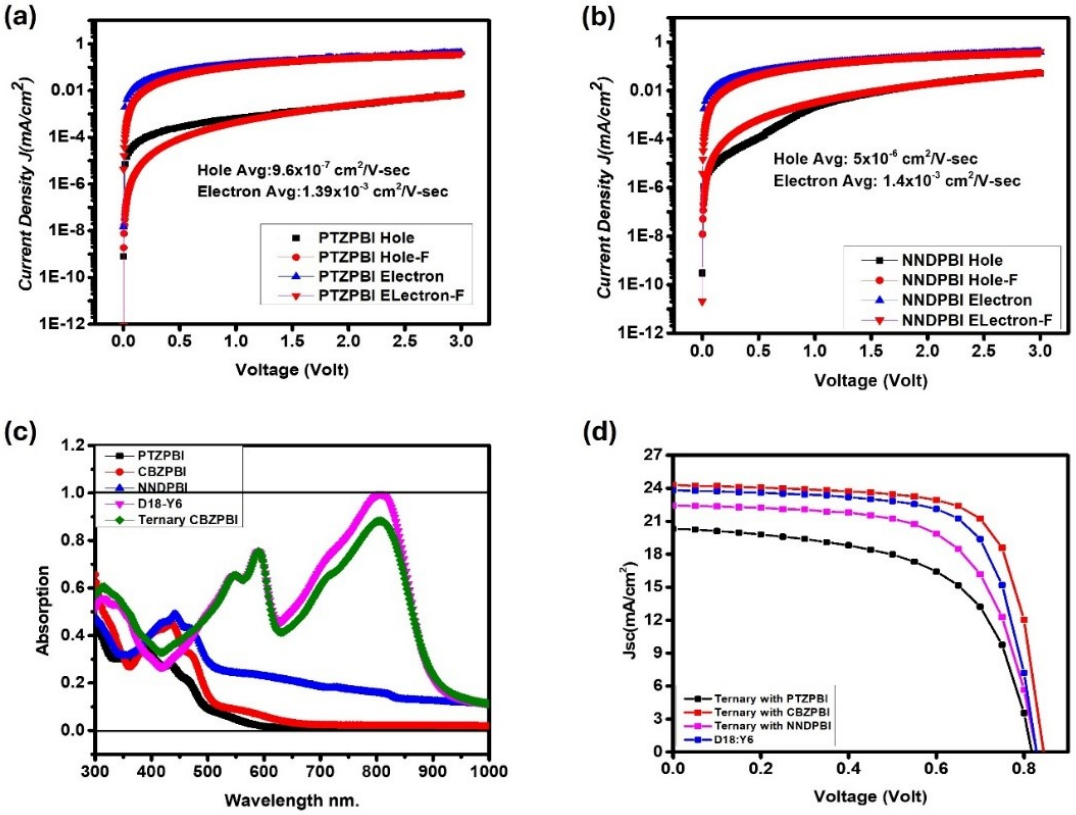

Figure S2: (a) Carrier mobility plot of **PTZPBI** compound (b) Carrier mobility plot of **NNDPBI** compound (c) The absorption graph of all 3 PBI's compounds with **D18:Y6** film (d) The *J-V* graph under light of D18:Y6 and ternary devices with all 3 PBI's compounds.

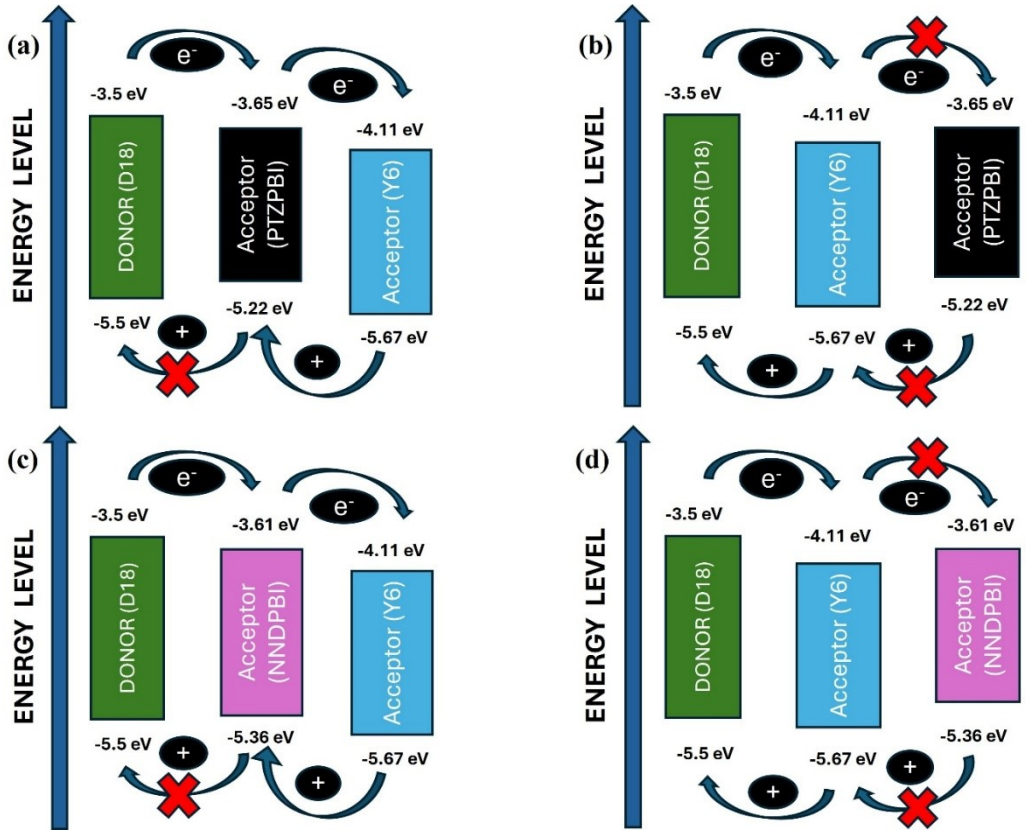

Figure S3: The energy alignment of **PTZPBI** and **NNDPBI** compounds with D18 donor and Y6 acceptor.

The field-dependent technique known as the space charge limited current (SCLC) method is used to measure the mobility. The *J-V* curve was obtained using a Keithley 2450 and a semi-log plot of *J-V* characteristics fitted with the modified Mott-Gurney equation (S1) to extract mobility.[1]

$$J = \frac{9}{8}\mu\varepsilon_r\varepsilon_o\frac{V^2}{d^3}\exp\left(0.891\gamma\sqrt{\frac{V}{d}}\right) \qquad (S1)$$

In the equation S1, J represents the measured current density (with a sample area of 6.0 mm²), ε_0 denotes the permittivity of free space, ε_r represents the relative dielectric constant of the material, V stands for the applied voltage, d indicates the thickness of the active layer of the material, μ signifies the mobility, and γ represents the fitting parameter that characterizes the

strength of the field dependence on mobility. The different devices were fabricated, *i.e*. single carrier device to measure the mobility of electrons and holes. Due to the limited intrinsic charge carriers in semiconductor materials, the devices were fabricated by sandwiching the materials between two conducting electrodes, acting a reservoir of the extrinsic carriers (with HOMO for hole-only devices and with LUMO for electron-only devices) under the application of suitable bias voltage. The alignment of energy levels of materials with electrode's work function (HOMO alignment for holes and LUMO alignment for electrons) is required to make an ohmic contact for efficient insertion of charge carriers.[2]

The electron and hole mobility device fabricated on ITO (Indium tin oxide) substrates. We started fabricating with properly cleaning of ITO (Indium tin oxide) coated glass substrate with ultra-sonication in 5% Hellmanex soap solution followed by DI (Deionised water), Acetone and IPA (2-Propanol) with 20 minutes each. Then substrates were blow dried with nitrogen gas and UV treated for 20 minutes at 70 °C. The two set of devices i.e. were prepared to measure the carrier mobility for electrons and holes respectively. The choice of electrodes and interlayers are to form near ohmic contact. The carrier mobility given in table S2 is the average data of 5 best devices. Keithley 2450 source meters is used to extract the J-V characteristics of the devices. The active area of each device was 6 mm^2. The dielectric constant was measured using an LCR meter. The thickness of each layer was extracted using a profilometer.

The hole only device with structure ITO/PEDOT: PSS /Material/ MoO_3/Ag was used to fabricate the hole only devices. The 35-40 nm layer of PEDOT: PSS 1000 spin-coating on top of cleaned ITO substrates with 100 µl of solution at 4500 rpm for 45 seconds and annealed at 140 °C for 20 minutes. PBI's series acceptor materials **PTZPBI**, **CBZPBI**, and **NNDPBI** solution in chloroform (10mg/ml) stirred overnight was spin-coated on PEDOT: PSS coated substrate at 1000 rpm for 30 seconds to obtained a thickness of around 100nm and D18:Y6 and ternary solution (D18:Y6: **CBZPBI** (20%)) also spin coated on PEDOT: PSS coated substrate

at 2500 rpm for 30 seconds to obtained a uniform thickness of around ~100nm. Finally, 7 nm of MoO_3 and 100 nm of Ag were evaporated onto the active layer using a thermal evaporator through a metal mask of area 6 mm^2.

The electron only device with structure ITO/ZnO /Material /PDINN/Al was used to fabricate electron only devices. The ZnO sol-gel solution was prepared by vigorously stirring 200 mg of Zinc Dihydrate in 52 mg of ethanolamine and 2 ml of 2-Methoxyethanol overnight at room temperature. A 30-35 nm layer of ZnO was deposited by spin-coated of ZnO solution on cleaned ITO substrates at 4000 rpm for 60 seconds. Subsequently, annealed at 180°C for 1 hour in ambient conditions. The solution of active materials PBI's materials (**PTZPBI**, **CBZPBI**, and **NNDPBI**) prepared in chloroform (10mg/ml) was spin-coated on ZnO coated substrate at 1000 rpm for 30 seconds and D18:Y6 binary and ternary solution (D18:Y6: **CBZPBI** (20%)) spin coated on ZnO coated substrate at 2500 rpm for 30 seconds to obtained a uniform thickness of around ~100nm. A thin layer of a PDINN was deposited by spin-coating of 1 mg/ml solution in methanol at a rate of 2000 rpm for 30 seconds dynamically. Finally, 100 nm thermally evaporated Aluminium electrode was grown on top of PDINN layer through metal mask of area 6 mm^2.

The carrier mobility of **PTZPBI** and **NNDPBI** material is illustrated in **Figure S2** and carrier mobility for **CBZPBI** and D18:Y6 base devices with ternary devices represented in **Figure 9** of main text.

Table S2: Charge carrier mobility data (best of five devices) of all 3 PBI's compounds **PTZPBI**, **CBZPBI**, **NNDPBI**, and D18:Y6 with D18: Y6: **CBZPBI** (20%) devices.

PTZPBI	**Hole Mobility (cm^2 V^{-1} s^{-1}) (10^{-7})**	**Electron Mobility (cm^2 V^{-1} s^{-1}) (10^{-3})**
1	3.83	2.0

2	3.33	0.86
3	8.1	2.1
4	23	1.4
5	10	0.6
Average	**9.67**	**1.39**
STDEV	**7.1**	**0.69**

CBZPBI	**Hole Mobility** *(cm² V⁻¹ s⁻¹)* ×10⁻⁷	**Electron Mobility** **(cm² V⁻¹ s⁻¹)** ×10⁻³
1	9.0	1.2
2	3.3	1.1
3	8.6	0.92
4	0.62	1.08
5	0.94	1.5
Average	**4.5**	**1.16**
STDEV	**3.6**	**0.19**

NNDPBI	**Hole Mobility (cm² V⁻¹ s⁻¹)** **(10⁻⁶)**	**Electron Mobility (cm² V⁻¹ s⁻¹)** **(10⁻³)**
1	3.8	1.3
2	7.5	1.45
3	7.5	2.5
4	3.2	1.59
5	3.2	0.22
Average	**5.0**	**1.4**

STDEV	**2.0**	**0.72**

D18:Y6	**Hole Mobility (cm^2 V^{-1} s^{-1}) (10^{-4})**	**Electron Mobility (cm^2 V^{-1} s^{-1}) (10^{-4})**
1	8.5	2.9
2	5.0	4.6
3	14	2.3
4	5.0	2.45
5	8.3	5.0
Average	**8.2**	**2.95**
STDEV	**3.2**	**0.84**

Ternary (D18:Y6: CBZPBI 20%)	**Hole Mobility (cm^2 V^{-1} s^{-1}) (10^{-4})**	**Electron Mobility (cm^2 V^{-1} s^{-1}) (10^{-4})**
1	35.8	2.0
2	2.0	3.4
3	3.36	9.4
4	4.0	2.0
5	1.65	8.6
Average	**9.4**	**5.0**

STDEV	**13**	**3.2**

The stability of **D18:Y6** and **D18:Y6: CBZPBI (20%)** devices was studied by regularly measuring the devices for more than 900 hrs, when stored under a controlled environment with a humidity of 35±10%. The effect of incorporation of 20% **CBZPBI** in ternary devices is significant as the ternary devices retained 80% of their PCE for more than 700 hrs, but the PCE of base devices reduced below the 80% mark in less than 550 hrs **Figure S4 c**. Thus, it proves that adding **CBZPBI** helps the device increase its performance and maintain its original yield. We all know that fabricating the OSCs devices in inert conditions avoids the effect of water vapours and oxygen. So, to study the impact of water vapours, we measured the contact angle of the base device and 20% **CBZPBI**-based ternary device to study its hydrophobic nature. The contact angle measurement with DI water formed an angle of 76.3° in ternary devices, **Figure S4 b**, whereas the base device made an angle of 68.3° **Figure S4 a**. The increased angle clearly shows the superior water resistance property of ternary-based devices compared to base devices, ultimately leading to a stable performance for a longer duration.[3]

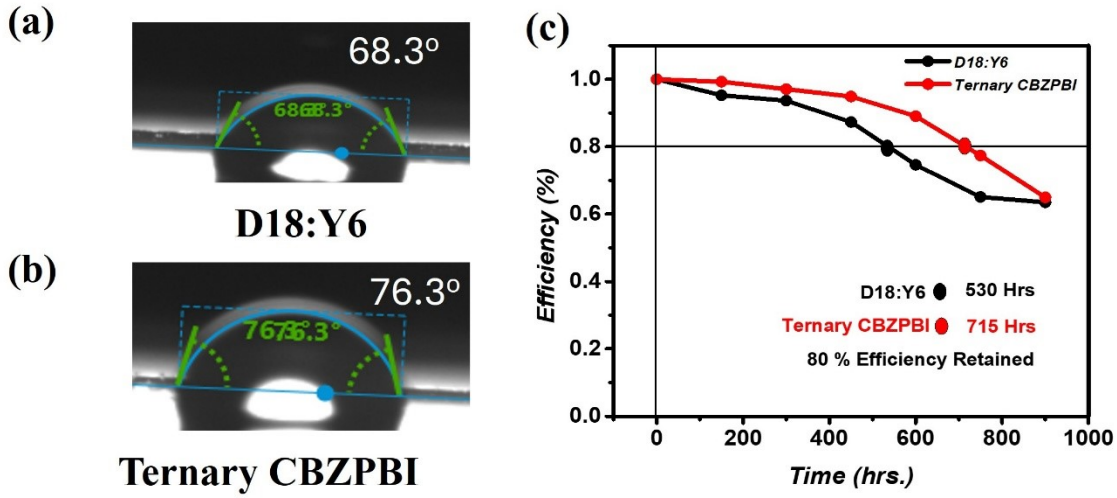

Figure S4: (a) Contact angle for D18:Y6 thin film with DI water. (b) Contact angle for D18:Y6: **CBZPBI** (20%) thin film with DI water (c) Stability data of D18:Y6 and D18:Y6: **CBZPBI** (20%) OSCs devices.

Synthesis details

Synthesis of PTZPBI:

A degassed solution of PDI-NH_2 (100 mg, 10.16 mmol, 1 equiv.) and PTZ-CHO (171 mg, 0.15878 mmol, 4 equiv.) in toluene (10 mL) was prepared, followed by the addition of trifluoroacetic acid (TFA, 100 µL). The reaction mixture was heated at 110 ºC for 1-2 hours under a nitrogen atmosphere. After completion, the solvent was removed under reduced pressure, and the crude residue was purified by column chromatography on silica gel using a DCM/hexane (90:10) eluent. Compound **1** appeared as a purple solid. The obtained purple residue (**1**) was dissolved in dichloromethane (CH_2Cl_2, 150 mL) and stirred at room temperature under visible light exposure (white LED, 7 W) for 3-4 hours, during which the solution gradually turned green. Subsequently, DDQ (30 mg, 2 equiv.) was added, and the reaction mixture was stirred at room temperature for 10–15 minutes. The solvent was then removed under vacuum, and the crude product was purified by column chromatography, followed by precipitation from CH_2Cl_2/MeOH, affording **PTZPBI** as a brown solid., ^{1}H NMR of (**1**) (500 MHz, $CDCl_3$) δ = 8.90 (d, *J* = 8.2 Hz, 1 H), 8.52–8.47 (m, 2 H), 8.47– 8.38 (m, 3 H), 8.35 (d, *J* = 8.1 Hz, 1 H), 8.06 (s, 1 H), 7.82–7.73 (m, 2 H), 7.25–7.17 (m, 2 H), 7.05–6.97 (m, 2 H), 6.93 (d, *J* = 8.1 Hz, 1 H), 4.14 (dd, *J* = 8.2, 12.7 Hz, 2 H), 4.08 (dd, *J* = 6.6, 12.6 Hz, 2 H), 3.92 (t, *J* = 7.0 Hz, 2 H), 2.02–1.85 (m, 4 H), 1.47–1.37 (m, 8 H), 1.33 (br. s., 8 H), 1.10 (t, *J* = 7.3 Hz, 3 H), 0.99–0.93 (m, 6 H), 0.90 (d, *J* = 4.6 Hz, 6 H), **^{13}C{^{1}H} NMR** (125 MHz ,$CDCl_3$) δ = 190.0, 150.8, 143.4, 131.0, 130.0, 128.4, 127.6, 127.5, 125.0, 123.8, 123.6, 116.0, 114.8, 49.8, 49.7, 37.9, 30.8, 29.7, 28.8, 28.7, 24.1, 23.1, 20.2, 20.1, 14.2, 11.3, 11.2, 10.6., **MS (MALDI-TOF)**: calcd for Chemical Formula: $C_{56}H_{56}N_4O_4S$: 880.40, found = 880.3897.,

^{1}H NMR of (**PTZPDI)** (500 MHz, $CDCl_3$) δ = 9.55 (br. s., 1 H), 9.38 (br. s., 1 H), 9.10 (br. s., 2 H), 9.04 (br. s., 1 H), 8.96 (d, *J* = 7.0 Hz, 1 H), 7.81 (br. s., 2 H), 7.20 (br. s., 3 H), 6.95 (s, 1 H), 7.00 (s, 1 H), 4.31–4.16 (m, 4 H), 4.13–3.83 (m, 2 H), 2.03 (br. s., 4 H), 1.51–1.42 (m, 8 H), 1.35 (br. s., 8 H), 1.13 (br. s., 3 H), 1.01–0.96 (m, 6 H), 0.92–0.88 (m, 6 H) **^{13}C{^{1}H} NMR** (125 MHz, $CDCl_3$) δ = 190.04, 150.76, 143.43, 131.05, 130.05, 127.57, 123.58, 115.98, 114.82, 49.71, 23.12, 20.06, 14.16, 11.21, 10.64., **MS (MALDI-TOF)**: calcd for Chemical Formula: $C_{56}H_{54}N_4O_4S$: 878.39, found = 878.3416.

Compound CBZPBI. A degassed solution of PDI-NH_2 (100 mg, 0.15878 mmol, 1 equiv.) and CBZ-CHO (93 mg, 0.47634 mmol, 3 equiv.) in toluene (10 mL) was prepared, followed by the addition of trifluoroacetic acid (TFA, 100 μL). The reaction mixture was heated at 110 °C for 1-2 h under a nitrogen atmosphere. Upon completion, the solvent was removed under reduced pressure, and the residue was purified by silica gel column chromatography using dichloromethane/hexane (90:10, v/v) as the eluent, affording compound **2** as a purple solid. Compound **2** was dissolved in dichloromethane (150 mL) and stirred at room temperature under visible light irradiation (white LED, 7 W) for 3-4 h, during which the solution gradually changed from purple to green. DDQ (30 mg, 2 equiv.) was then added, and the mixture was stirred for an additional 10–15 min at room temperature. The solvent was removed under reduced pressure, and the crude product was purified by column chromatography, followed by precipitation from CH_2Cl_2/MeOH, to yield **CBZPBI** as a brown solid. **^{1}H NMR** (400 MHz ,$CDCl_3$) δ = 10.08 (s, 1 H), 9.48 (s, 1 H), 9.12 (s, 1 H), 8.76 (br. s., 2 H), 8.66 (s, 2 H), 8.69 (s, 1 H), 8.58 (br. s., 1 H), 8.26 (d, J = 6.8 Hz, 1 H), 8.18–8.05 (m, 1 H), 7.98 (d, J = 8.5 Hz, 1 H), 7.55–7.52 (m, 1 H), 7.47 (t, J = 8.2 Hz, 2 H), 7.30 (d, J = 6.8 Hz, 1 H), 4.36–4.27 (m, 2 H), 4.18 (m, 4 H), 2.03 (br. s., 2 H), 1.96–1.91 (m, 2 H), 1.46 (br. s., 8 H), 1.38–1.31 (m, 8 H), 1.00 (d, J = 7.3 Hz, 9 H), 0.91 (d, J = 6.3 Hz, 6 H), **^{13}C{^{1}H} NMR** (125 MHz, $CDCl_3$) δ = 163.6, 163.4, 162.2, 143.2, 141.1, 133.7, 131.3, 130.9, 127.5, 126.8, 126.3, 124.3, 123.5, 122.9, 122.5,

121.0, 120.2, 109.7, 109.3, 45.9, 44.9, 44.2, 38.0, 37.9, 30.8, 30.3, 29.7, 28.8, 28.7, 24.1, 24.0, 23.1, 22.4, 14.2, 11.8, 11.7, 10.6, 8.7. **MS (MALDI-TOF)**: calcd for $C_{56}H_{57}N_4O_4$: 849.44, found: 849.4008., **^{1}H NMR** (125 MHz, $CDCl_3$) δ = 9.46 (s, 1 H), 9.08 (s, 1 H), 8.77–8.72 (m, 1 H), 8.72–8.66 (m, 2 H), 8.63 (br. s., 1 H), 8.62 (br. s., 1 H), 8.26 (d, *J* = 7.6 Hz, 1 H), 7.98–7.89 (m, 1 H), 7.46 (dd, *J* = 3.4, 8.2 Hz, 2 H), 7.29 (t, *J* = 7.3 Hz, 2 H), 4.29–4.08 (m, 6 H), 2.02 (td, *J* = 5.9, 12.1 Hz, 2 H), 1.96–1.89 (m, 2 H), 1.53–1.43 (m, 8 H), 1.42–1.29 (m, 8 H), 1.07–0.96 (m, 9 H), 0.91 (d, *J* = 7.3 Hz, 6 H), **^{13}C{^{1}H} NMR** (125 MHz, $CDCl_3$) δ = 163.3, 163.1, 163.0, 162.7, 161.6, 143.3, 140.9, 140.9, 133.6, 132.7, 132.4, 130.8, 129.2, 128.6, 128.2, 128.1, 127.4, 126.7, 126.0, 125.0, 124.7, 123.5, 123.5, 123.0, 122.7, 122.6, 122.2, 122.0, 121.4, 121.2, 121.1, 121.0, 121.0, 119.4, 116.4, 108.8, 108.7, 44.5, 44.4, 38.0, 37.9, 30.8, 30.7, 29.7, 28.7, 26.9, 24.0, 24.0, 23.2, 23.2, 22.2, 14.2, 11.8, 10.6, 10.6., **MS** (**MALDI-TOF**): calcd for $C_{56}H_{54}N_4O_4$: 846.41 found = 846.3890.

Synthesis of NNDPBI: A degassed solution of PDI-NH_2 (100 mg, 0.15878 mmol, 1 equiv.) and CBZ-CHO (71 mg, 0.6351 mmol, 4 equiv.) in toluene (10 mL) was prepared, followed by the addition of trifluoroacetic acid (TFA, 100 μL. The reaction mixture was heated at 110 °C for 1-2 hours under a nitrogen atmosphere. Upon completion, the solvent was evaporated under reduced pressure, and the crude residue was purified by column chromatography on silica gel using DCM/hexane (90:10) as the eluent, yielding compound **3** as a purple solid. The obtained purple residue **3** was dissolved in dichloromethane (CH_2Cl_2, 150 mL) and stirred at room temperature under visible light exposure (white LED, 7 W) for 3–4 hours, during which the solution gradually turned green. Subsequently, DDQ (30 mg, 2 equiv.) was added, and the reaction mixture was stirred at room temperature for another 10–15 minutes. The solvent was then removed under vacuum, and the crude product was purified by column chromatography, followed by precipitation from CH_2Cl_2/MeOH, affording **NNDPBI** as a brown solid, **^{1}H NMR**

(500 MHz, CDCl3) δ = 9.22 (d, *J* = 8.5 Hz, 1 H), 8.67–8.58 (m, 3 H), 8.58–8.50 (m, 3 H), 8.25 (s, 1 H), 7.95 (d, *J* = 8.5 Hz, 2 H), 6.87 (d, *J* = 8.5 Hz, 2 H), 4.23–4.07 (m, 4 H), 3.18 (s, 6 H), 1.97 (br. s., 2 H), 1.42 (d, *J* = 4.5 Hz, 8 H), 1.36–1.30 (m, 8 H), 1.00–0.94 (m, 6 H), 0.93–0.85 (m, 6 H). **^{13}C{^{1}H} NMR** (125 MHz, $CDCl_3$) δ = 163.7, 163.5, 160.8, 153.3, 150.4, 134.6, 133.7, 131.6, 131.2, 131.0, 129.9, 128.7, 128.4, 125.9, 124.3, 123.6, 122.9, 122.5, 122.4, 121.6, 121.1, 111.9, 111.0, 44.2, 40.2, 40.1, 38.0, 37.9, 30.8, 30.8, 28.8, 28.7, 24.1, 24.1, 23.1, 14.2, 10.6., **MS (MALDI-TOF)**: calcd for $C_{49}H_{53}N_4O_4$: 760.40. found: 760.4357., **^{1}H NMR** for (**NNDPBI**) (500 MHz, $CDCl_3$) δ = 9.46 (s, 1 H), 9.17 (s, 1 H), 8.90–8.87 (m, 2 H), 8.84–8.82 (m, 2H), 7.91–7.83 (m, *J* = 8.5 Hz, 2 H), 7.00–6.95 (m, *J* = 8.5 Hz, 2 H), 4.15 (t, *J* = 8.2 Hz, 4 H), 3.12 (s, 6 H), 1.38 (td, *J* = 6.7, 13.2 Hz, 8 H), 1.29 (br. s., 8 H), 1.18 (s, 3 H), 0.95–0.88 (m, 6 H), 0.84 (t, *J* = 6.8 Hz, 6 H)., **^{13}C{^{1}H} NMR** (125 MHz, $CDCl_3$) δ = 163.4, 163.3, 163.2, 162.9, 160.9, 151.5, 143.7, 133.8, 132.7, 132.6, 132.5, 130.9, 129.4, 128.1, 127.9, 126.9, 125.3, 125.0, 124.8, 122.8, 122.3, 122.2, 122.1, 121.7, 121.6, 121.0, 120.8, 116.4, 112.6, 44.6, 44.4, 40.4, 38.0, 37.9, 30.8, 30.7, 28.7, 28.7, 24.0, 24.0, 23.2, 14.2, 10.6. **MS (MALDI-TOF)**: calcd for $C_{49}H_{50}N_4O_4$: 758.38. found (M+H) 759.3130.

Characterization

^{1}H-NMR, **^{13}C-NMR**, **MALDI of PDI derivatives**.

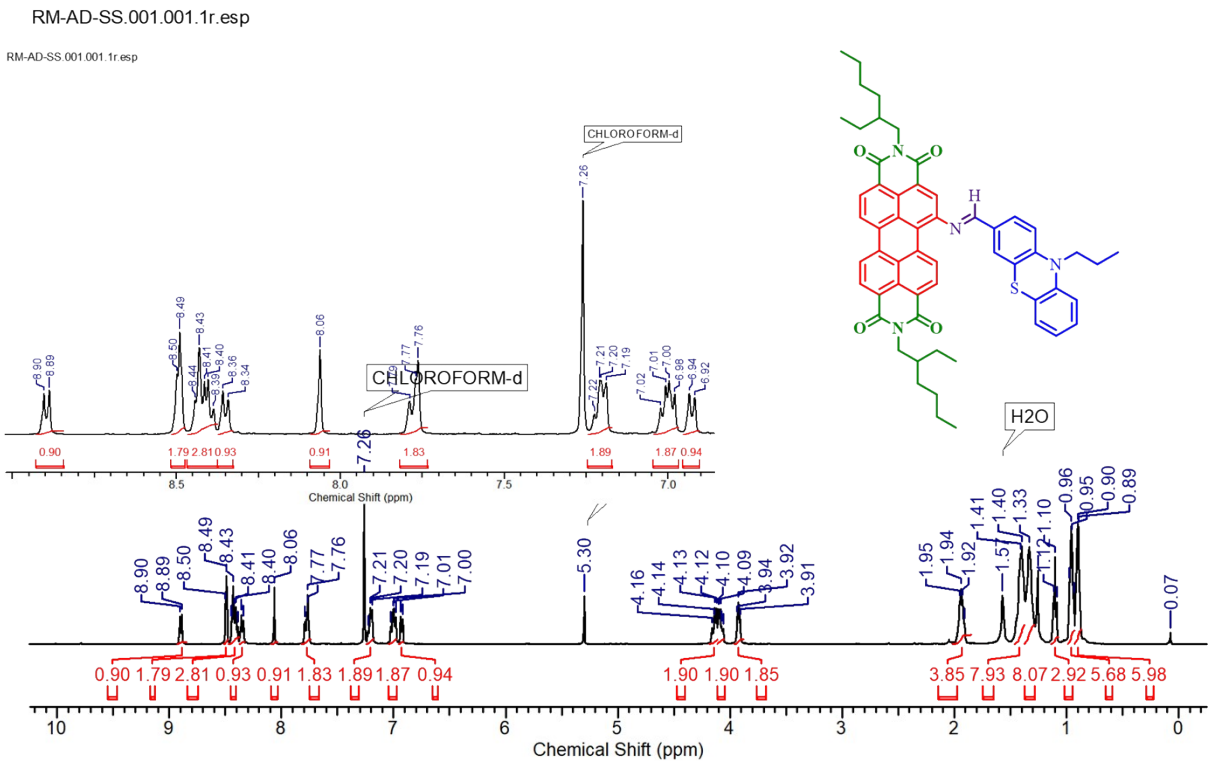

Figure S5. ^{1}H NMR of compound **1**.

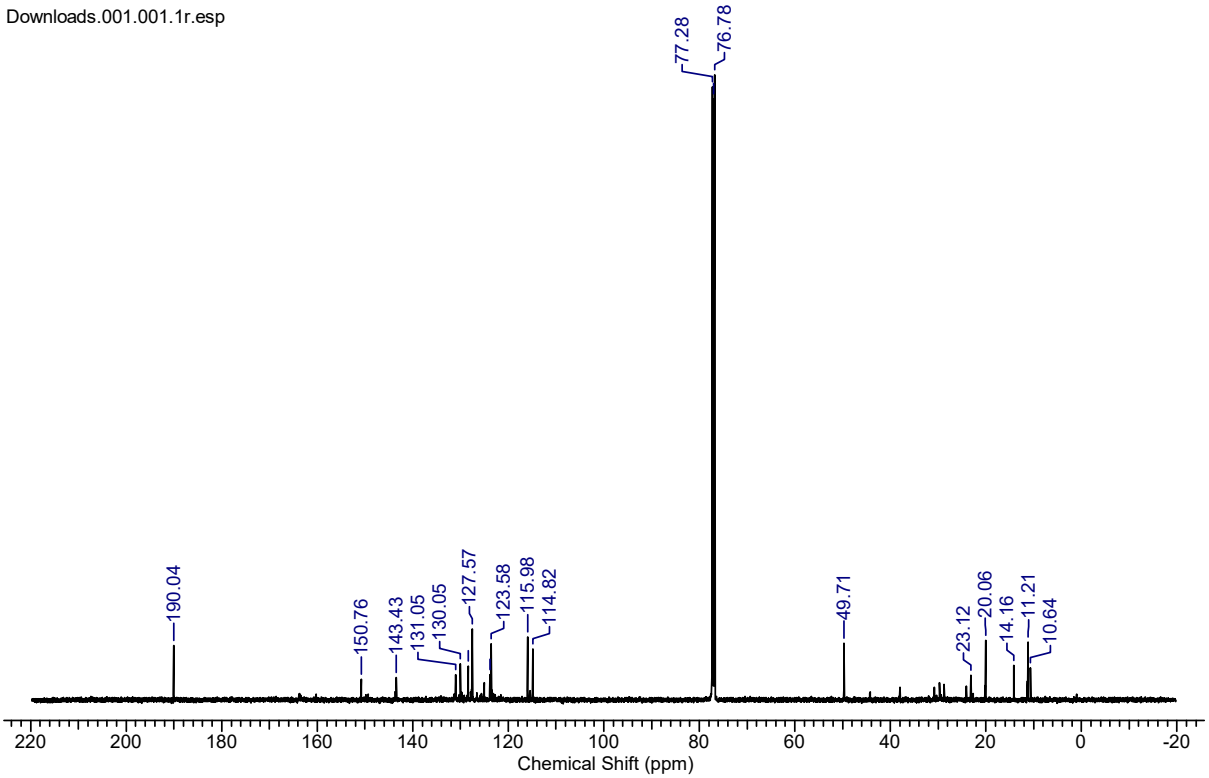

Figure S6. ^{13}C NMR of compound **1**.

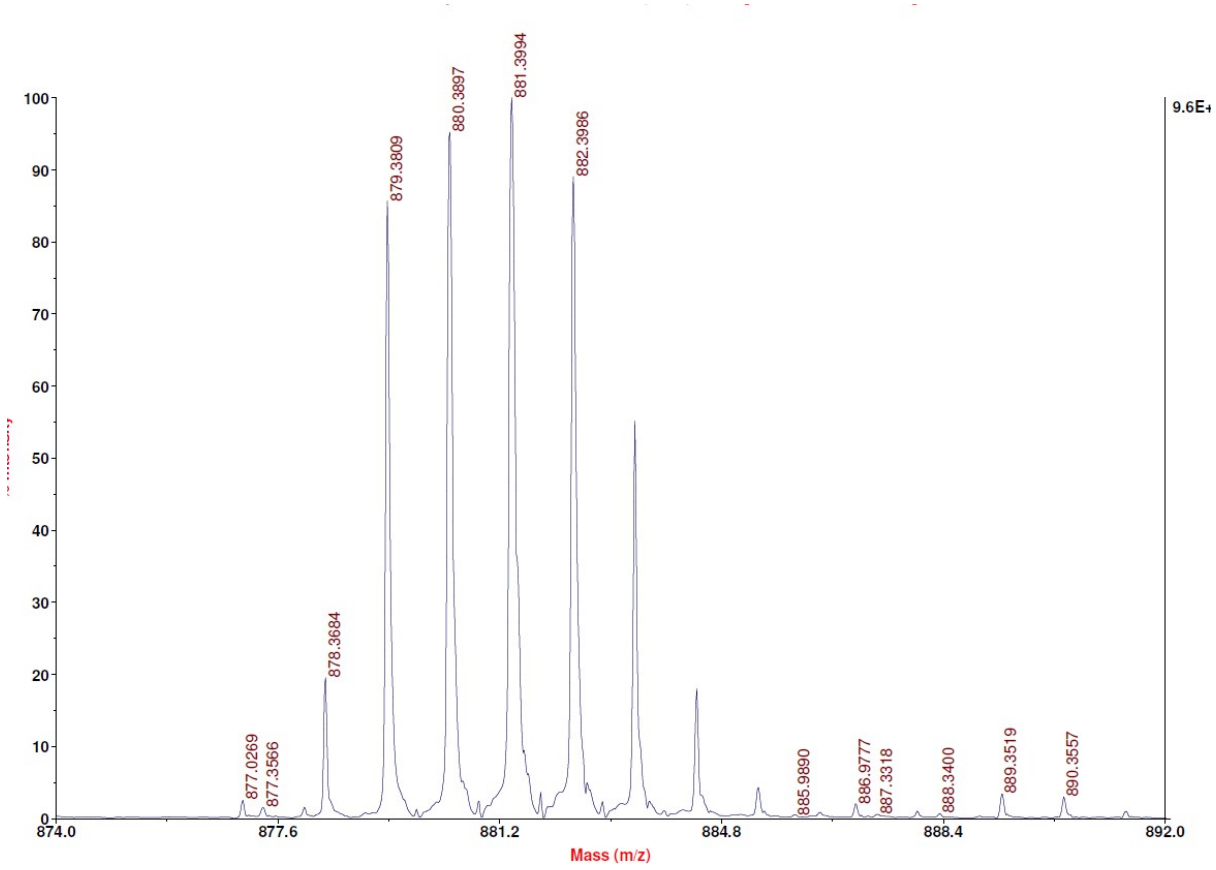

Figure S7. MALDI of compound **1**.

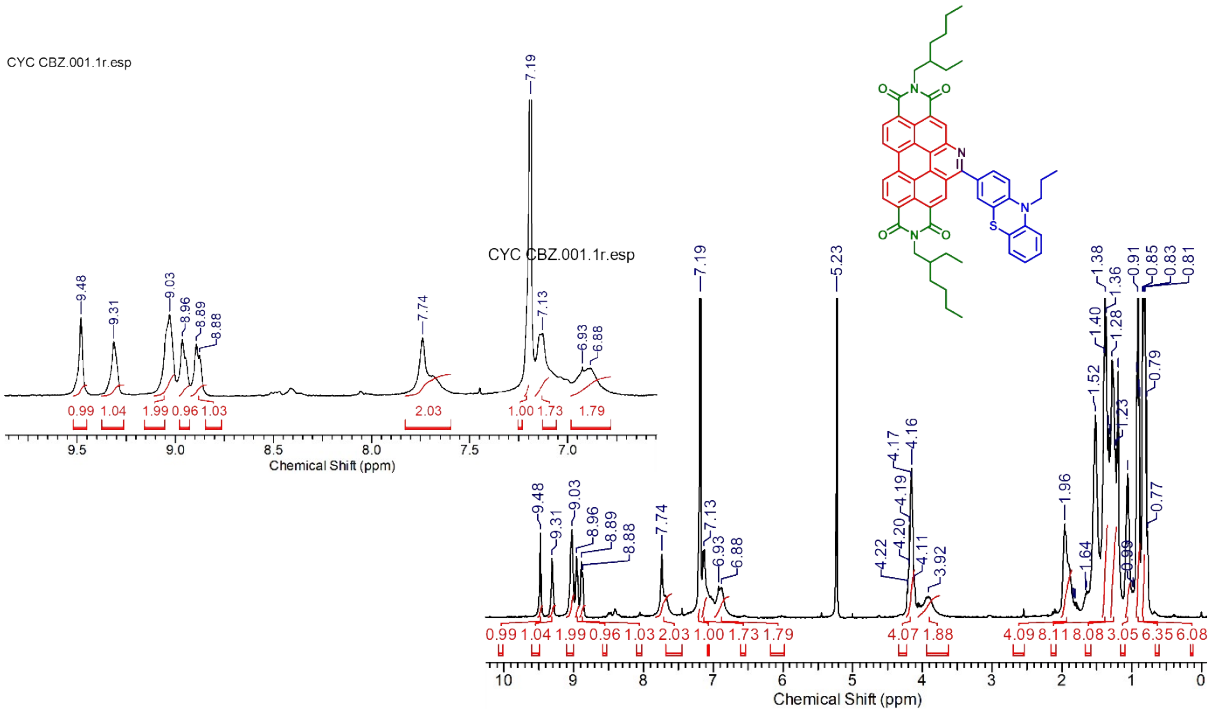

Figure S8. ^{1}H NMR of compound **PTZPBI**.

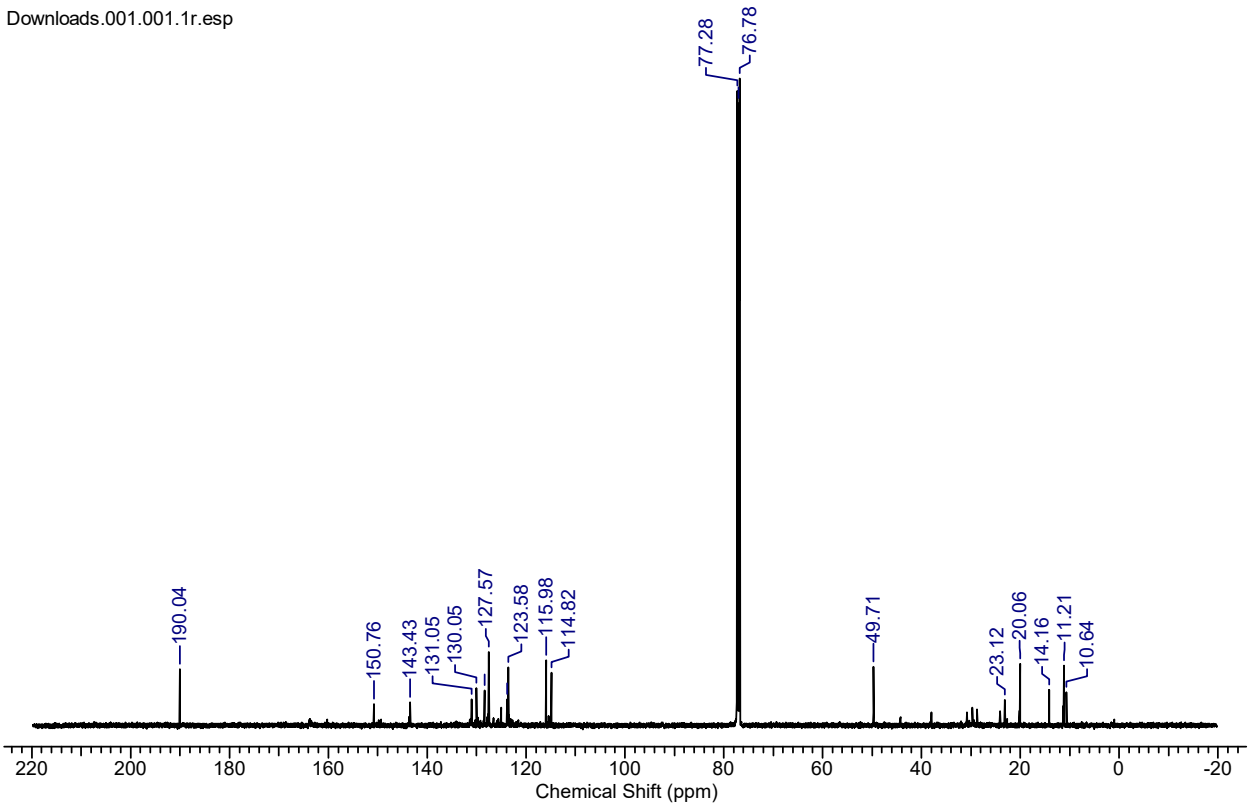

Figure S9. ^{13}C NMR of compound **PTZPBI**.

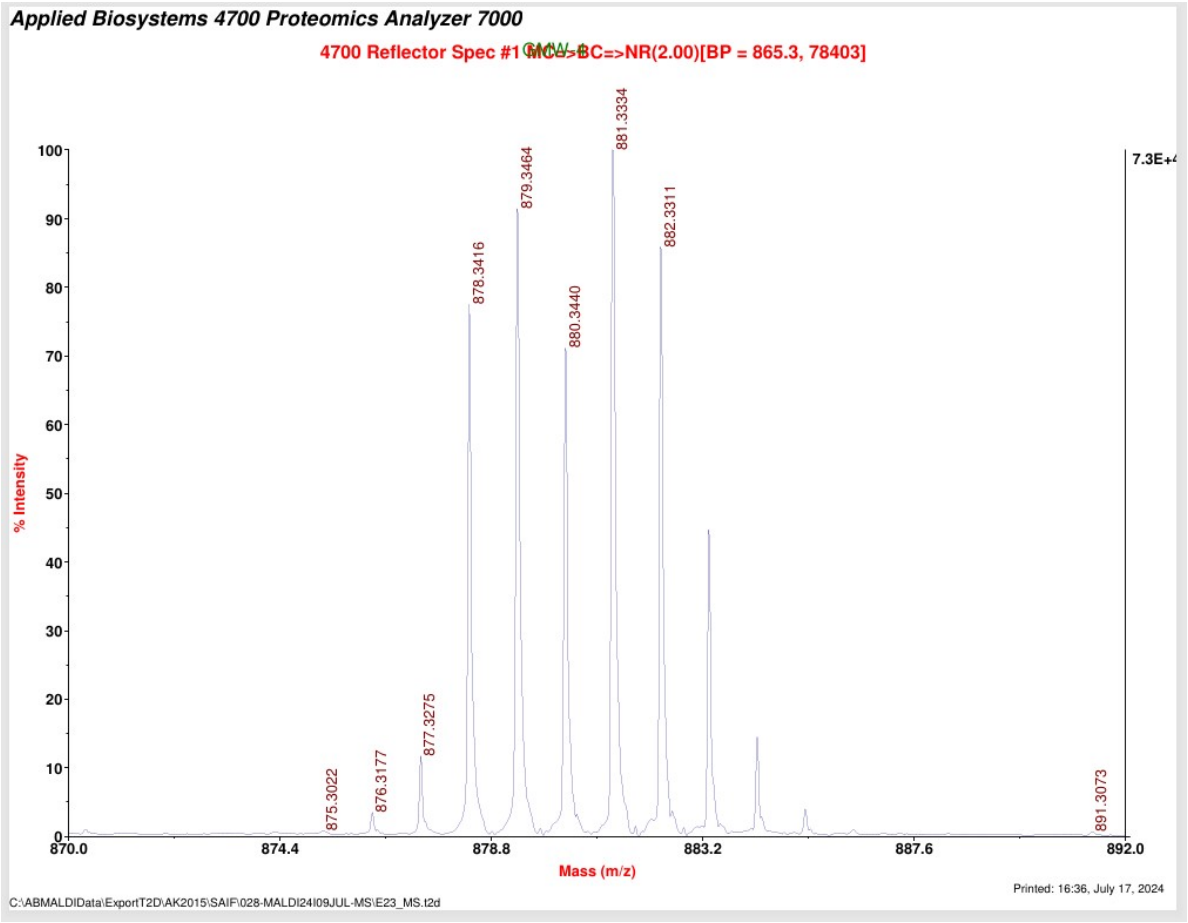

Figure S10. MALDI of compound **PTZPBI**.

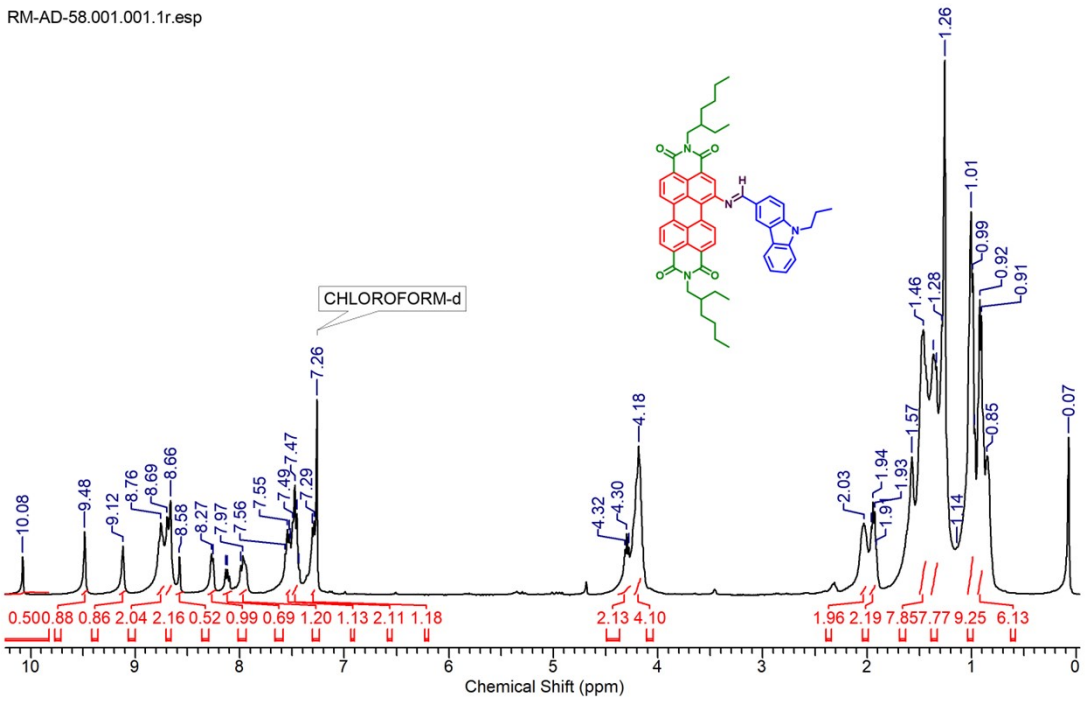

Figure S11. ^{1}H NMR of compound **2**.

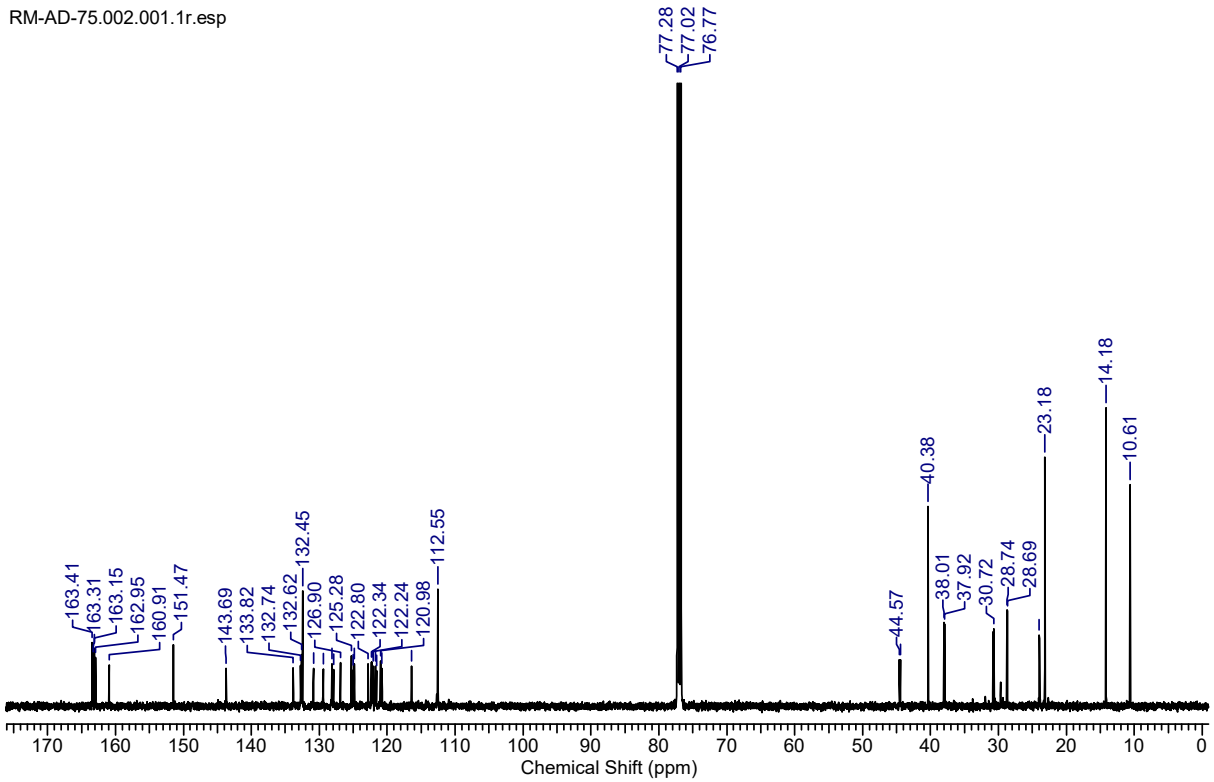

Figure S12. ^{13}C NMR of compound **2**.

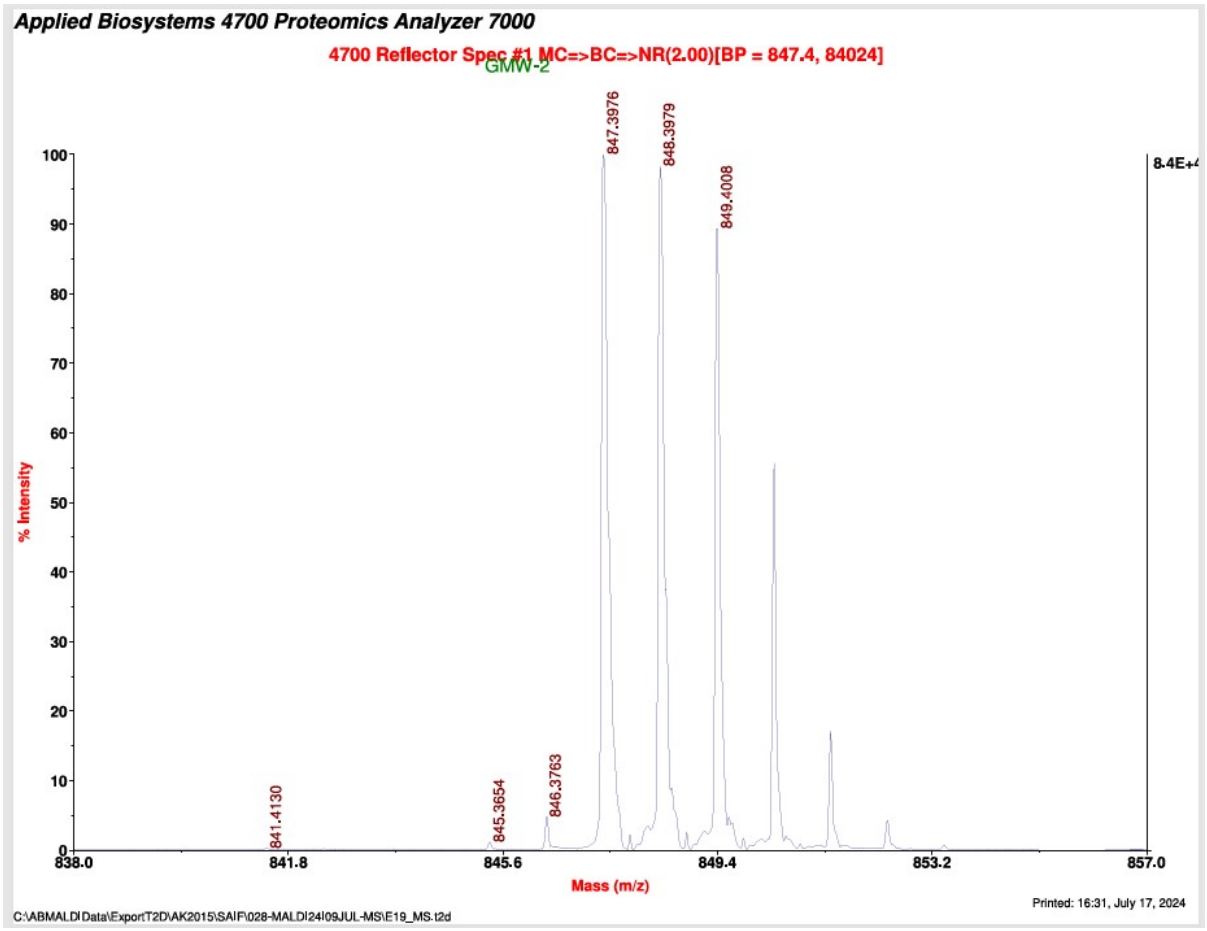

Figure S13. MALDI of compound **2**.

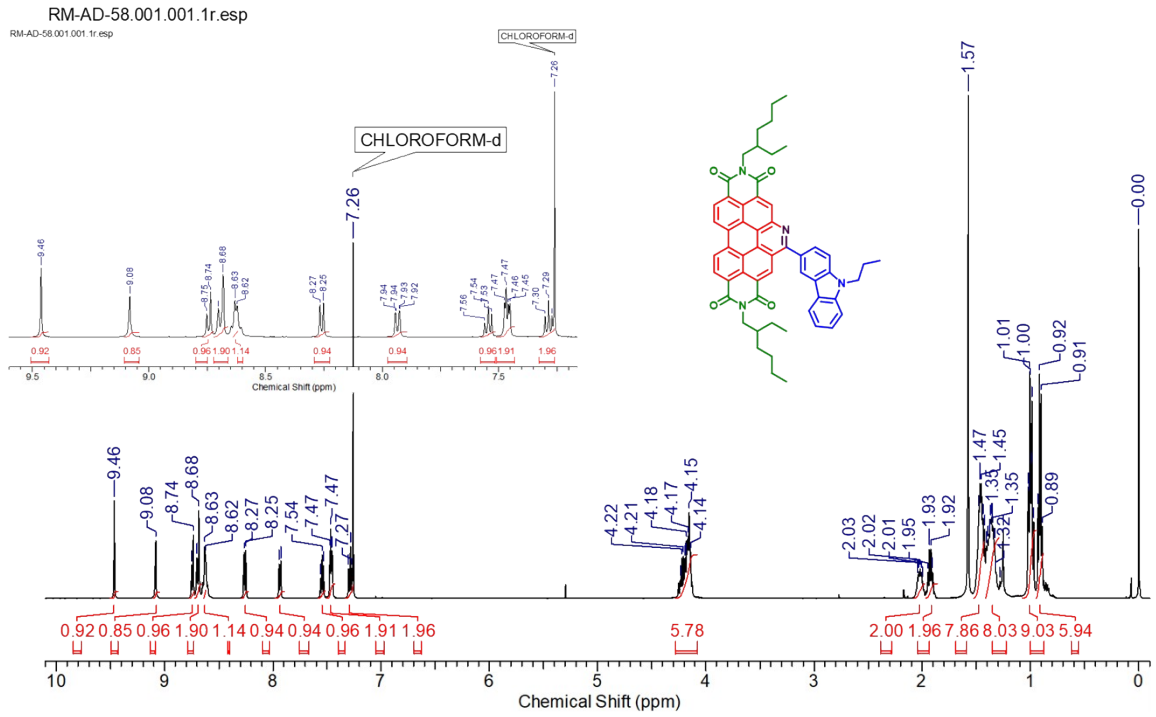

Figure S14. ^{1}H NMR of compound **CBZPBI**.

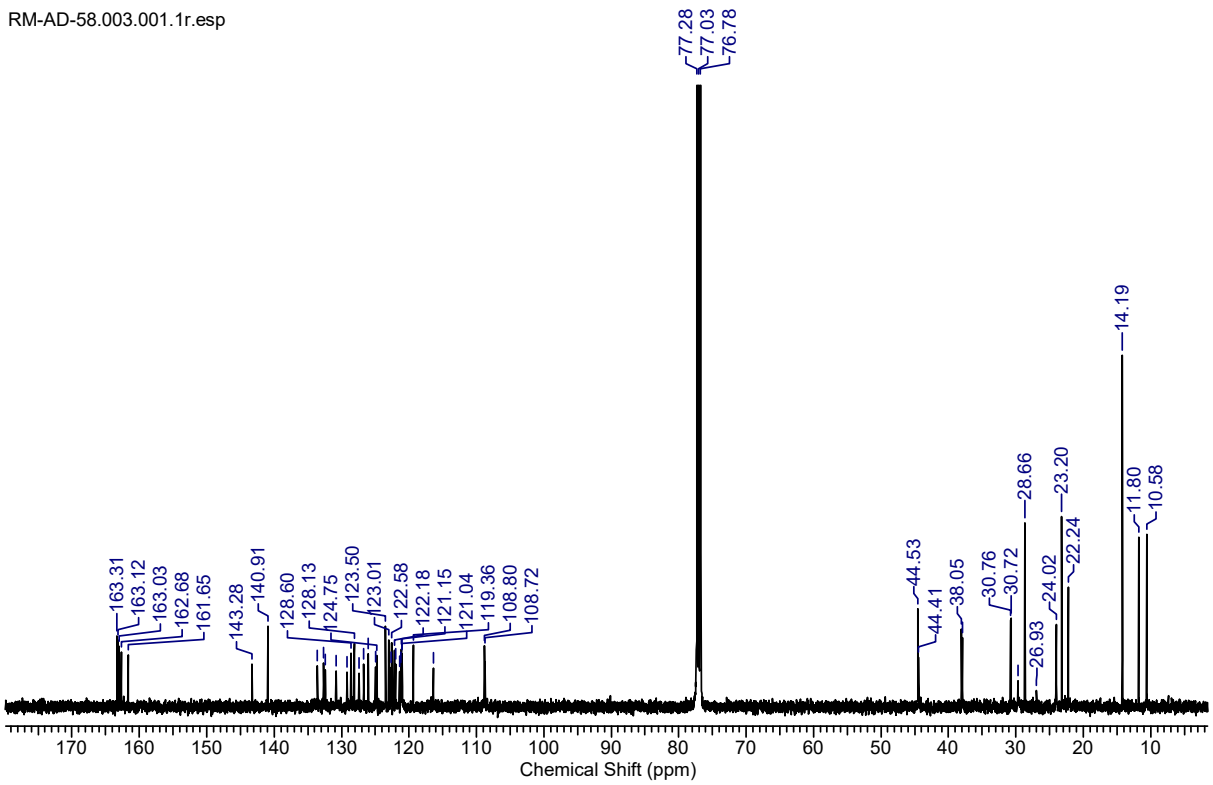

Figure S15. ^{13}C NMR of compound **CBZPBI**.

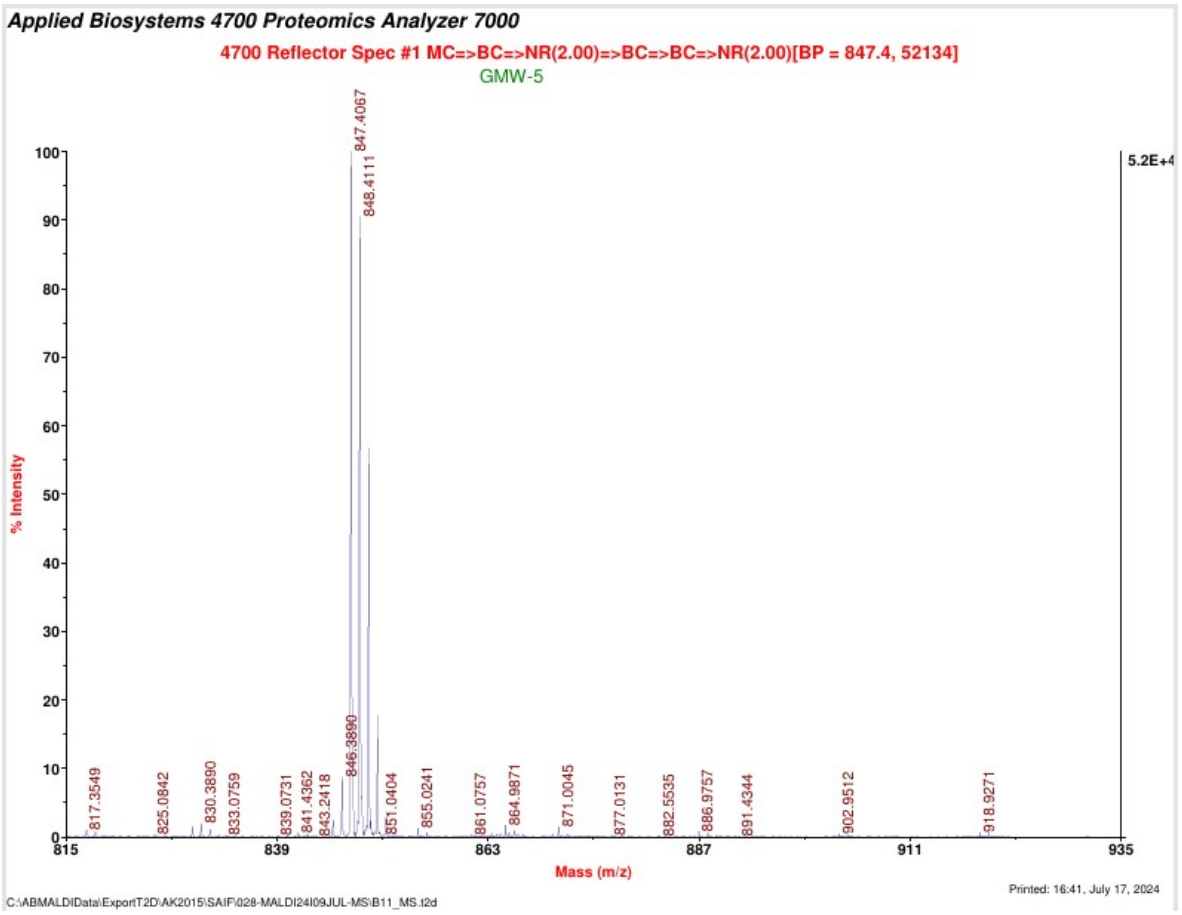

Figure S16. MALDI of compound **CBZPBI**.

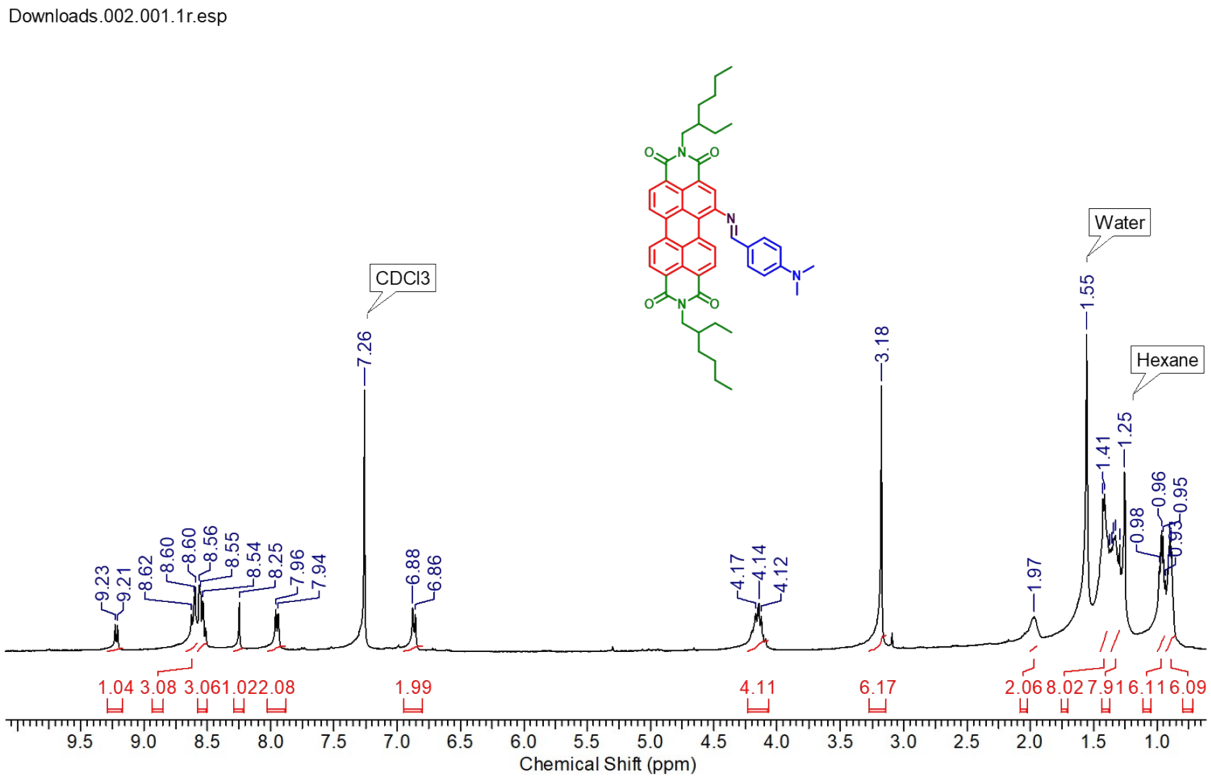

Figure S17. ^{1}H NMR of compound **3**.

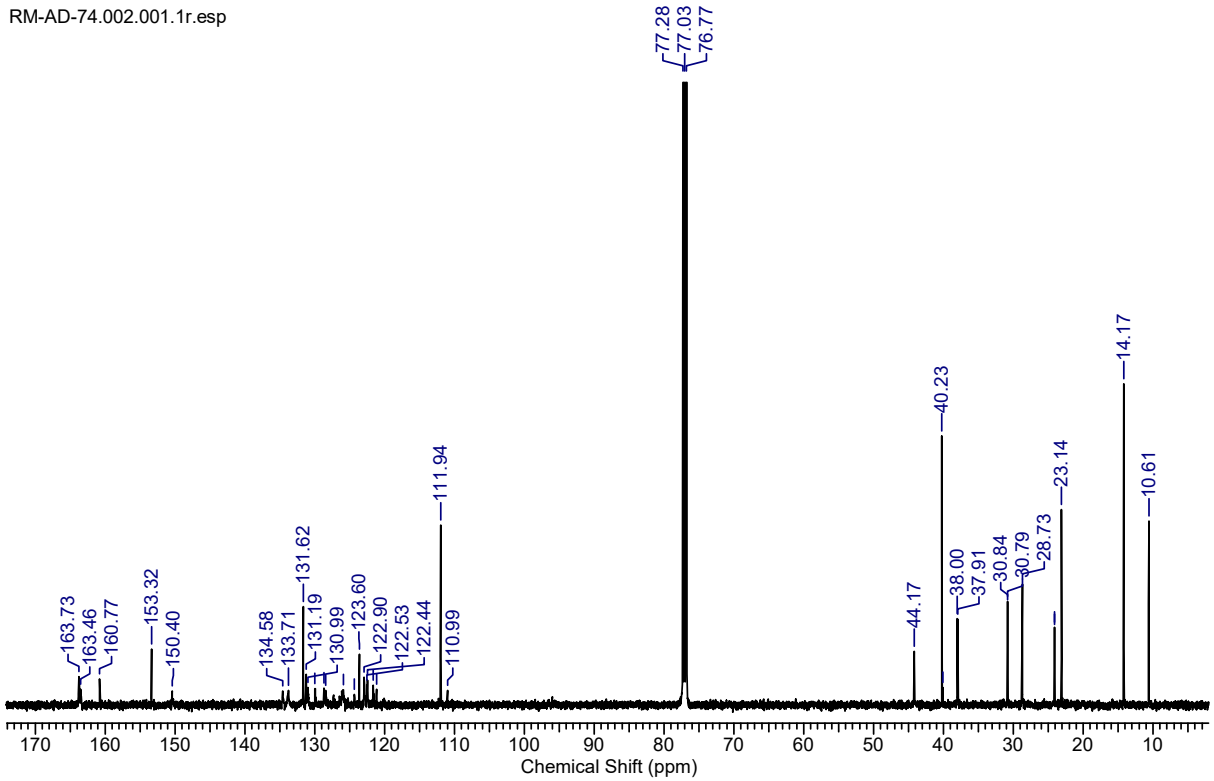

Figure S18. ^{13}C NMR of compound **3**.

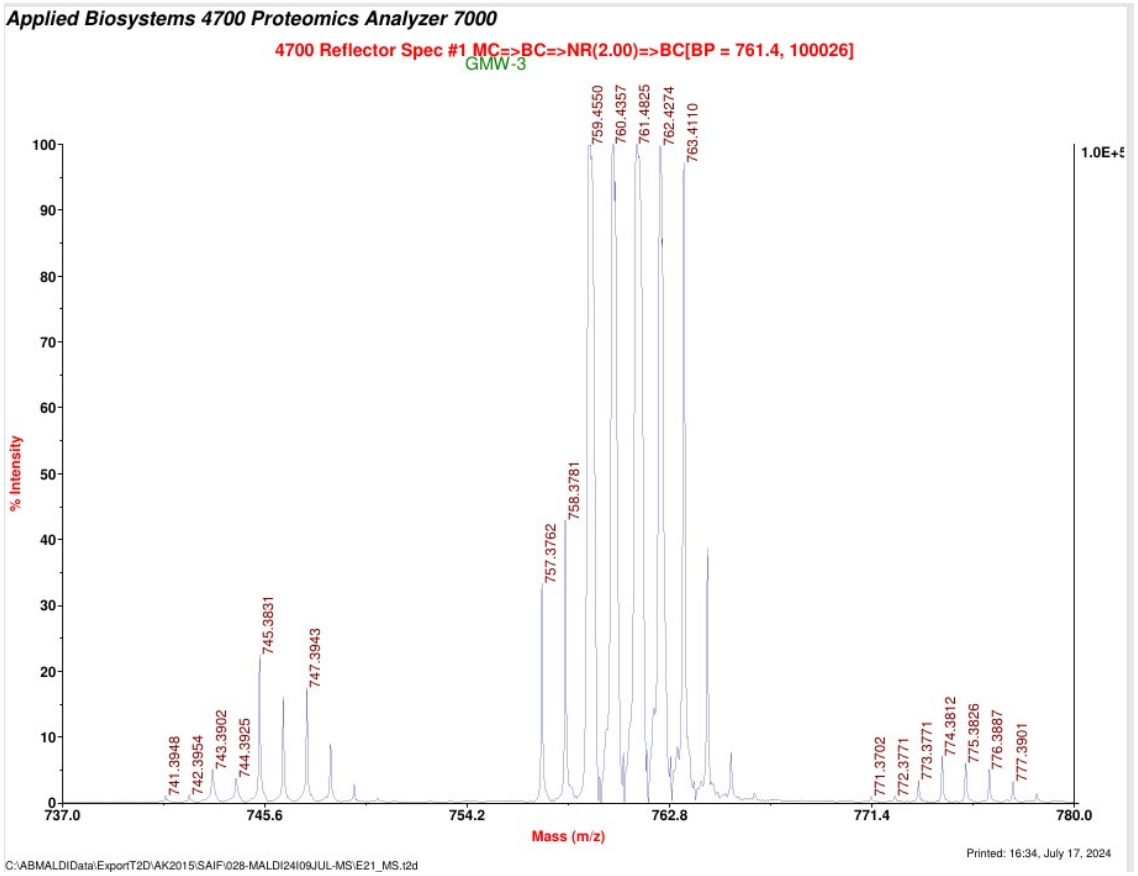

Figure S19. MALDI of compound **3**.

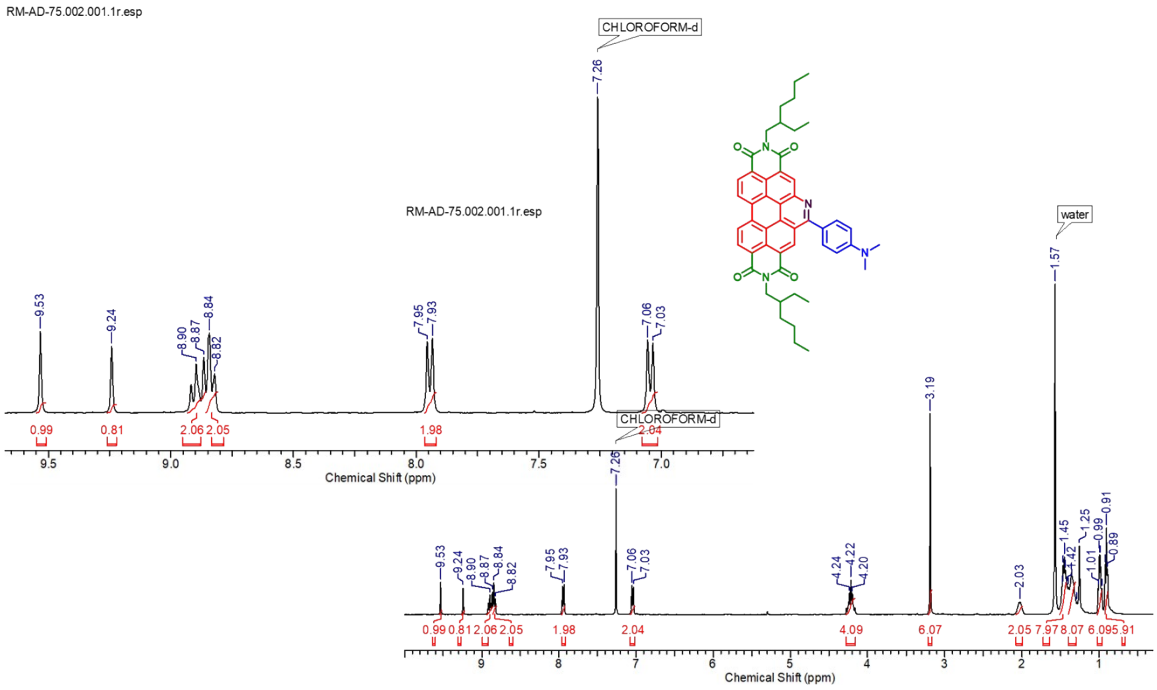

Figure S20. ^{1}H NMR of compound **NNDPBI**.

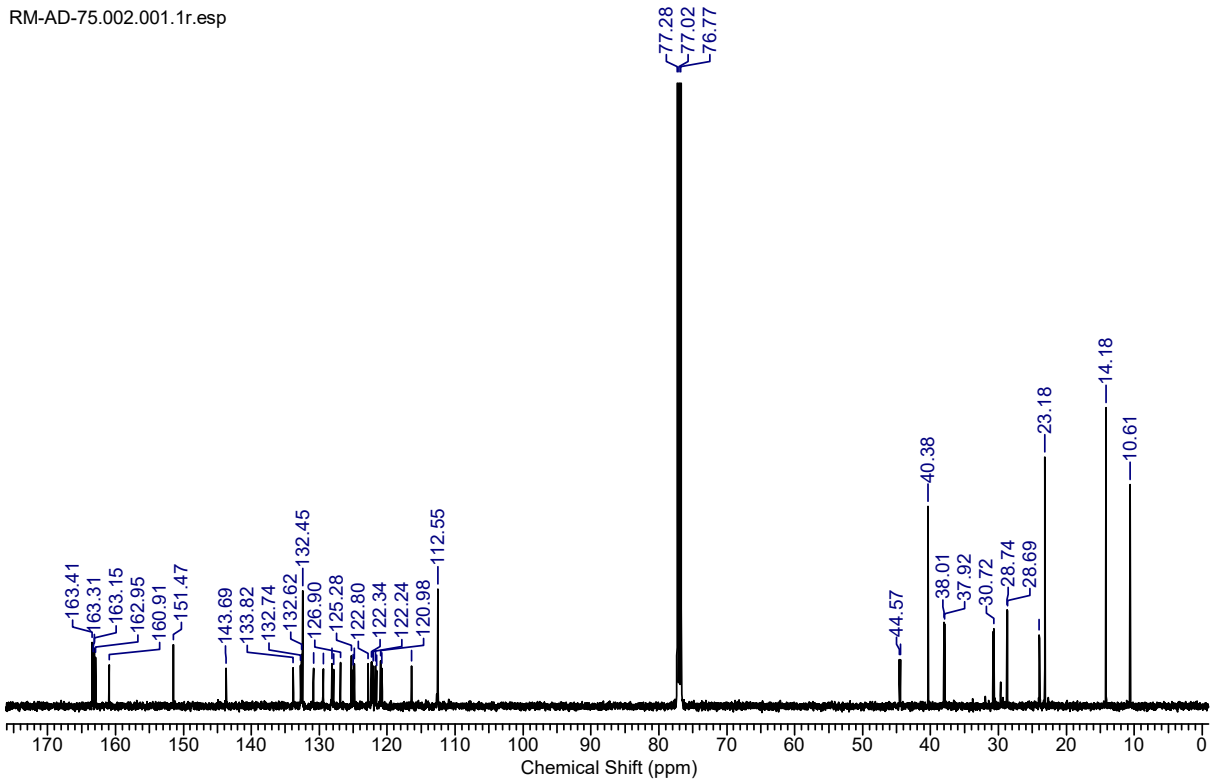

Figure S21. ^{13}C NMR of compound **NNDPBI**.

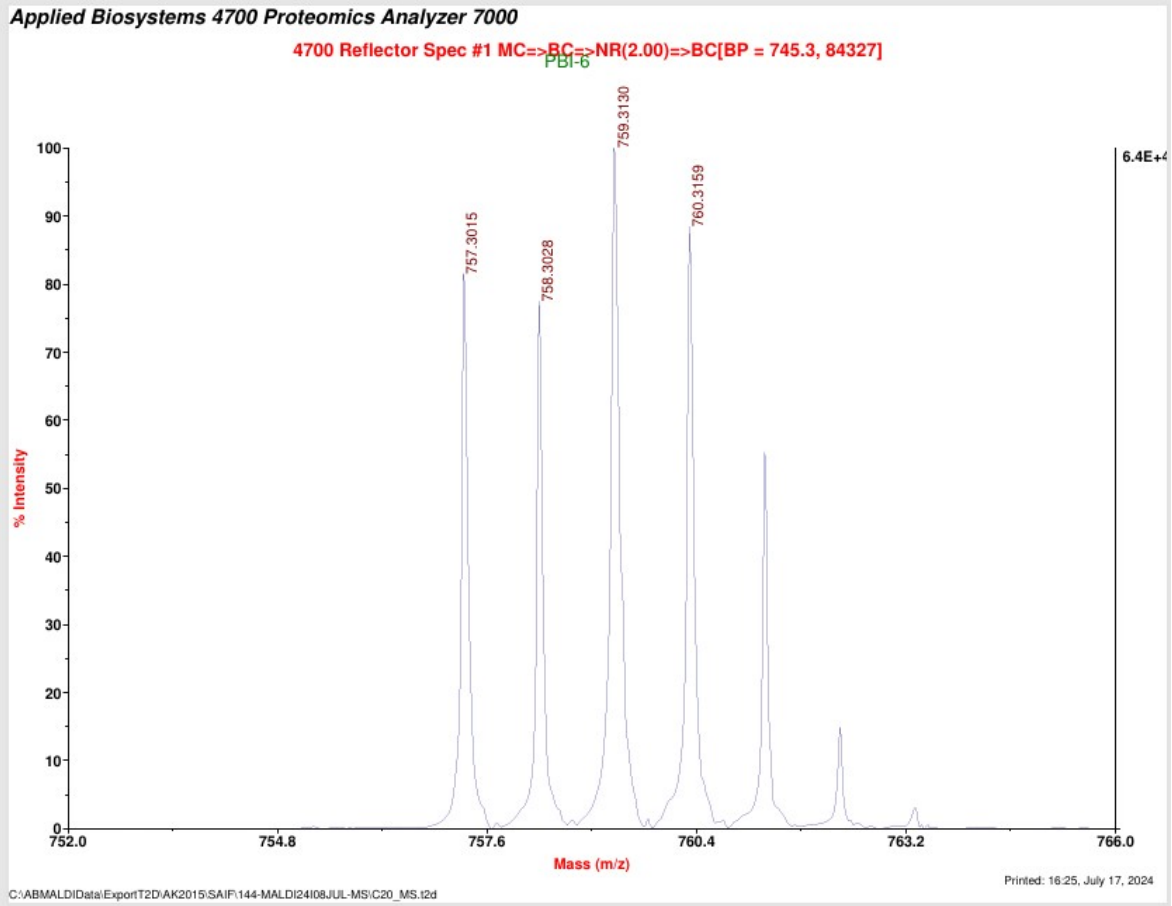

Figure S22. MALDI of compound **NNDPBI**.

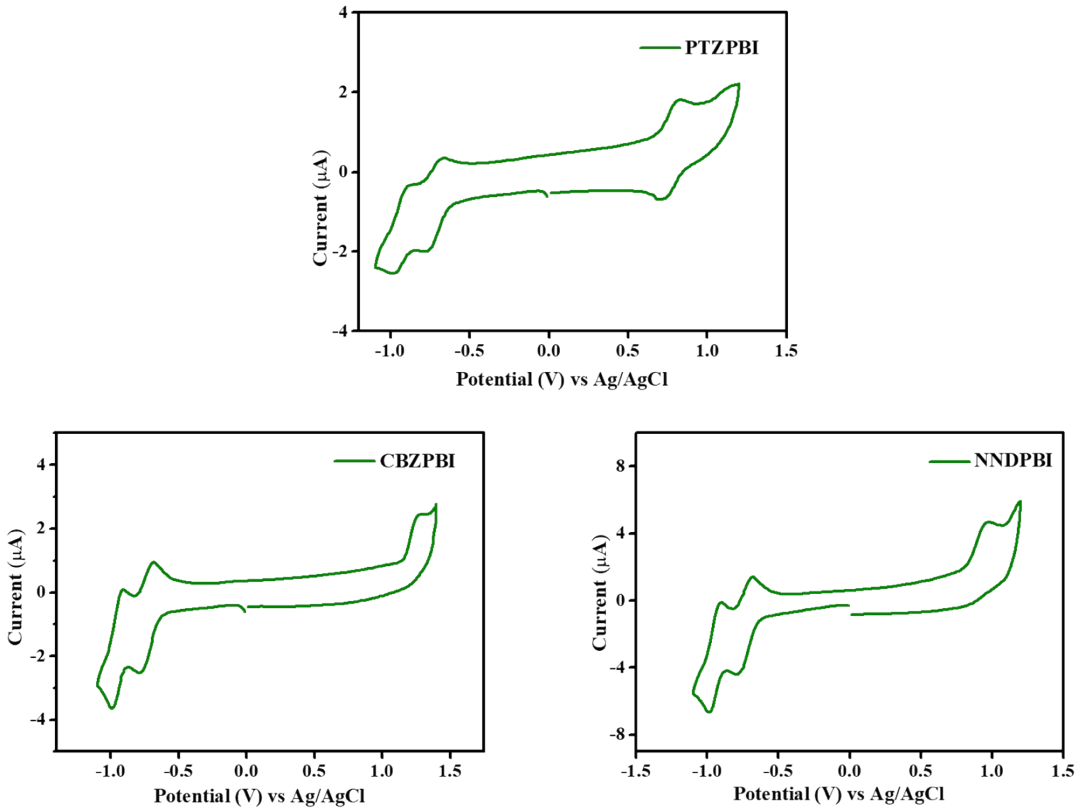

Figure S23. Cyclic voltammograms showing the oxidation and reduction potentials of **PTZPBI**, **CBZPBI**, and **NNDPBI** were recorded in dichloromethane (DCM) using 0.1 M tetrabutylammonium perchlorate as the supporting electrolyte at a scan rate of 100 mV s^{-1} versus Ag/AgCl at 25 °C.

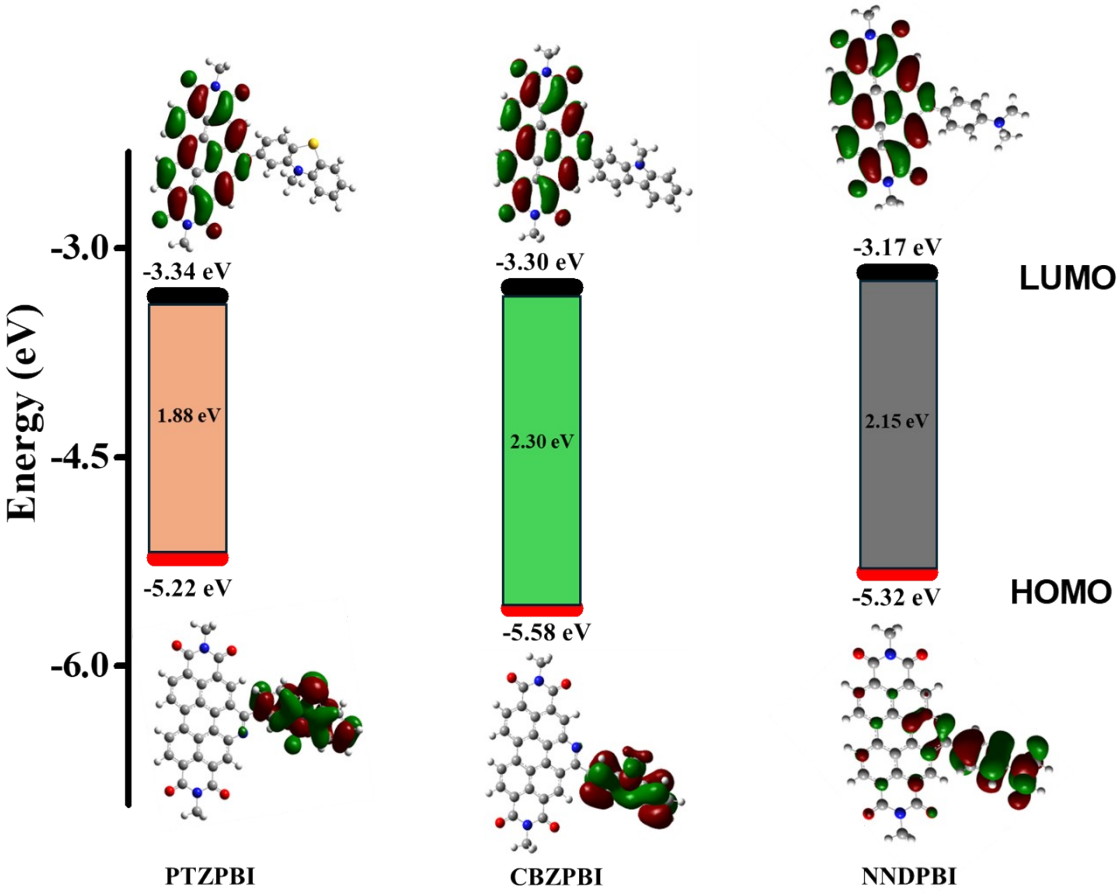

Figure S24. Energy diagram and frontier molecular orbitals of **PTZPBI**, **CBZPBI**, and **NNDPBI**.

DFT calculation:

The computational study was performed by using the Gaussian 09W program.[4]

DFT of compound (1)

Standard orientation:

Center Number	Atomic Number	Atomic Type	Coordinates (Angstroms) X	Y	Z
1	6	0	2.796372	-0.039805	0.061055
2	6	0	2.821155	-1.097312	0.983153
3	6	0	3.970928	0.310962	-0.626910
4	6	0	4.006403	-1.788238	1.198618
5	6	0	5.163027	-0.397690	-0.441362
6	1	0	3.939709	1.150094	-1.312937
7	6	0	5.164959	-1.461494	0.486674
8	1	0	4.042858	-2.600718	1.917583
9	7	0	6.335900	-0.091516	-1.163844
10	6	0	7.589254	-0.149033	-0.507652
11	6	0	6.217276	0.745149	-2.348374

12	6	0	7.850668	-1.182596	0.411667
13	6	0	8.596693	0.797271	-0.746269
14	1	0	6.107285	1.817165	-2.125069
15	1	0	7.106574	0.610717	-2.966700
16	6	0	9.836322	0.693883	-0.112482
17	1	0	8.418015	1.622703	-1.425015
18	6	0	10.082858	-0.330597	0.797685
19	1	0	10.603031	1.432207	-0.326382
20	1	0	11.042609	-0.407611	1.298039
21	1	0	5.350125	0.421111	-2.927581
22	1	0	1.917264	-1.353168	1.523917
23	6	0	9.076903	-1.259023	1.070134
24	1	0	9.244140	-2.058055	1.785926
25	6	0	1.579826	0.726792	-0.195725
26	1	0	1.676641	1.551205	-0.916761
27	7	0	0.454030	0.453057	0.361774
28	6	0	-0.657262	1.278821	0.188011
29	6	0	-1.970218	0.751640	0.052474
30	6	0	-0.456856	2.678377	0.254967
31	6	0	-3.068192	1.680190	0.035020

32	6	0	-2.268141	-0.683805	-0.085271
33	6	0	-1.498573	3.570825	0.173201
34	1	0	0.543200	3.070013	0.400694
35	6	0	-4.430636	1.237001	-0.000254
36	6	0	-2.824979	3.089488	0.067097
37	6	0	-3.635808	-1.122640	-0.029843
38	6	0	-1.281335	-1.659760	-0.274947
39	6	0	-1.201513	5.024919	0.225100
40	6	0	-5.453776	2.187236	-0.074244
41	6	0	-4.720834	-0.198460	0.050113
42	6	0	-3.891780	4.014904	0.010020
43	6	0	-3.930116	-2.522376	-0.068673
44	6	0	-1.583298	-3.025582	-0.331930
45	1	0	-0.250505	-1.361348	-0.366215
46	7	0	-2.302096	5.887977	0.147480
47	8	0	-0.058730	5.453505	0.324168
48	6	0	-5.196092	3.558334	-0.074364
49	1	0	-6.485314	1.864854	-0.139427
50	6	0	-6.025112	-0.690838	0.161920
51	6	0	-3.636577	5.474101	0.036979

52	6	0	-5.267165	-2.974961	0.030124
53	6	0	-2.886233	-3.469103	-0.213327
54	1	0	-0.795251	-3.758021	-0.468373
55	6	0	-2.068575	7.335692	0.183258
56	1	0	-6.001336	4.282162	-0.131060
57	6	0	-6.298423	-2.059558	0.157565
58	1	0	-6.858590	-0.006800	0.261164
59	8	0	-4.532703	6.305204	-0.030082
60	6	0	-5.584763	-4.422178	0.001922
61	6	0	-3.165259	-4.924575	-0.260690
62	1	0	-2.614076	7.776169	1.020037
63	1	0	-0.999276	7.495535	0.294309
64	1	0	-2.432270	7.792649	-0.739525
65	1	0	-7.314212	-2.428967	0.244463
66	7	0	-4.510348	-5.307831	-0.142937
67	8	0	-6.727796	-4.851218	0.097529
68	8	0	-2.276641	-5.756192	-0.393739
69	6	0	-4.841926	-6.736094	-0.175014
70	1	0	-5.511558	-6.942056	-1.012698
71	1	0	-3.912188	-7.288641	-0.282779

72	1	0	-5.353591	-7.017196	0.747682
73	16	0	6.625382	-2.451588	0.676863

Rotational constants (GHZ): 0.0661734 0.0308876 0.0214668

DFT of compound 2:

Standard orientation:

Center Number	Atomic Number	Atomic Type	Coordinates (Angstroms) X	Y	Z
1	6	0	-3.178327	0.592746	-0.071302
2	6	0	-3.336647	-0.465810	-0.999307
3	6	0	-4.286071	1.104076	0.623774
4	6	0	-4.583784	-1.019511	-1.237444
5	6	0	-5.535720	0.538279	0.382673
6	1	0	-4.155778	1.923629	1.324347
7	6	0	-5.701919	-0.522814	-0.551103
8	1	0	-4.695281	-1.828276	-1.953484

9	7	0	-6.768502	0.848026	0.942147
10	6	0	-7.732995	0.028535	0.368563
11	6	0	-7.020699	1.903433	1.900604
12	6	0	-7.107714	-0.848282	-0.559489
13	6	0	-9.112380	-0.012116	0.596078
14	1	0	-7.250101	2.859420	1.413860
15	1	0	-7.860687	1.624037	2.540415
16	6	0	-9.856404	-0.953270	-0.110448
17	1	0	-9.595509	0.665707	1.292024
18	6	0	-9.252102	-1.833093	-1.026889
19	1	0	-10.929396	-1.005059	0.048503
20	1	0	-9.864816	-2.552848	-1.560229
21	1	0	-6.145439	2.035761	2.540504
22	1	0	-2.458187	-0.825072	-1.522959
23	6	0	-7.881827	-1.785281	-1.256371
24	1	0	-7.417293	-2.462324	-1.967266
25	6	0	-1.867222	1.177772	0.188426
26	1	0	-1.848753	2.010379	0.906540
27	7	0	-0.787110	0.741419	-0.357718
28	6	0	0.432089	1.392666	-0.177893

29	6	0	1.651003	0.674354	-0.037220
30	6	0	0.445621	2.806846	-0.244411
31	6	0	2.876816	1.426066	-0.017471
32	6	0	1.728062	-0.789425	0.101700
33	6	0	1.610592	3.530393	-0.161354
34	1	0	-0.483602	3.345554	-0.390715
35	6	0	4.156352	0.781746	0.022534
36	6	0	2.849701	2.855864	-0.053288
37	6	0	3.013920	-1.430572	0.051351
38	6	0	0.604290	-1.605207	0.287450
39	6	0	1.544777	5.011123	-0.215101
40	6	0	5.310999	1.567110	0.095736
41	6	0	4.226564	-0.681184	-0.023710
42	6	0	4.043634	3.610787	0.002406
43	6	0	3.092875	-2.858732	0.090065
44	6	0	0.695982	-3.000898	0.343220
45	1	0	-0.370047	-1.154833	0.375000
46	7	0	2.758452	5.700998	-0.140078
47	8	0	0.489452	5.624559	-0.314230
48	6	0	5.263597	2.961133	0.090543

49	1	0	6.282212	1.093532	0.164055
50	6	0	5.442261	-1.365079	-0.127609
51	6	0	4.020066	5.093364	-0.030273
52	6	0	4.346800	-3.508213	-0.001888
53	6	0	1.917046	-3.636878	0.228129
54	1	0	-0.194686	-3.605322	0.475434
55	6	0	2.681998	7.165019	-0.184148
56	1	0	6.169325	3.554311	0.146364
57	6	0	5.505441	-2.759219	-0.122100
58	1	0	6.370043	-0.814950	-0.221907
59	8	0	5.042268	5.763725	0.032769
60	6	0	4.441803	-4.986564	0.025936
61	6	0	1.972168	-5.117523	0.271739
62	1	0	2.210914	7.482604	-1.116640
63	1	0	2.073809	7.528568	0.646718
64	1	0	3.695682	7.550949	-0.115202
65	1	0	6.454174	-3.278078	-0.203032
66	7	0	3.244837	-5.699672	0.161056
67	8	0	5.507549	-5.583660	-0.062174
68	8	0	0.967449	-5.806221	0.396166

69	6	0	3.356698	-7.161568	0.191665
70	1	0	3.982144	-7.467659	1.032936
71	1	0	2.353541	-7.567641	0.292444
72	1	0	3.826200	-7.515439	-0.728428

Rotational constants (GHZ): 0.0658955 0.0368615 0.0240617

DFT of compound 3:

Standard orientation:

Center Number	Atomic Number	Atomic Type	Coordinates (Angstroms) X	Y	Z
1	6	0	-4.593945	2.686703	-0.014301
2	6	0	-4.541887	1.293241	0.000564
3	6	0	-3.331755	0.592555	0.029927
4	6	0	-2.100543	1.325332	0.002841
5	6	0	-2.174232	2.753894	0.018279
6	6	0	-3.420019	3.421622	0.008218
7	6	0	-0.824621	0.662281	-0.027195
8	6	0	0.347621	1.466077	0.042494
9	6	0	0.233679	2.877564	0.093453
10	6	0	-0.982184	3.515672	0.058599
11	6	0	-3.296924	-0.870819	0.095071

12	6	0	-2.039036	-1.534513	-0.027994
13	6	0	-0.804983	-0.805275	-0.142180
14	6	0	-4.455679	-1.636598	0.262863
15	6	0	-4.420817	-3.031418	0.273874
16	6	0	-3.219038	-3.699588	0.107032
17	6	0	-2.019081	-2.965503	-0.048241
18	6	0	-0.798477	-3.661369	-0.229895
19	6	0	0.368972	-2.942401	-0.402608
20	6	0	0.365149	-1.543674	-0.364565
21	6	0	-1.019401	4.997771	0.092009
22	7	0	-2.281544	5.599136	0.062342
23	6	0	-3.500283	4.902515	0.018972
24	6	0	-3.211221	-5.180547	0.097810
25	7	0	-1.974322	-5.809846	-0.087081
26	6	0	-0.751049	-5.141749	-0.256448
27	8	0	-0.007842	5.686639	0.137344
28	8	0	-4.569412	5.498462	-0.006280
29	8	0	-4.226663	-5.850657	0.241606
30	8	0	0.293409	-5.761574	-0.416046
31	6	0	-2.307975	7.065345	0.083426
32	6	0	-1.984341	-7.275931	-0.100420
33	1	0	-5.540929	3.213962	-0.035796
34	1	0	-5.478674	0.750675	-0.017055
35	1	0	1.128048	3.482824	0.187143
36	1	0	-5.414448	-1.151297	0.395675

37	1	0	-5.326087	-3.614012	0.404219
38	1	0	1.293581	-3.485226	-0.565840
39	1	0	1.299858	-1.024376	-0.493710
40	1	0	-1.823193	7.431165	0.990947
41	1	0	-1.761625	7.457365	-0.776923
42	1	0	-3.348652	7.377204	0.051886
43	1	0	-2.648089	-7.633339	-0.890259
44	1	0	-0.965007	-7.611456	-0.273048
45	1	0	-2.357076	-7.653502	0.854254
46	6	0	3.992229	0.952066	-0.242586
47	6	0	4.310602	-0.065984	0.679193
48	6	0	5.046222	1.515306	-0.984197
49	6	0	5.610075	-0.502863	0.846933
50	1	0	3.509874	-0.504840	1.265546
51	6	0	6.354730	1.090904	-0.827513
52	1	0	4.830153	2.304671	-1.700286
53	6	0	6.676233	0.062563	0.095032
54	1	0	5.808569	-1.286846	1.566543
55	1	0	7.131343	1.555742	-1.421030
56	7	0	7.970247	-0.371885	0.257963
57	6	0	9.044789	0.225707	-0.519318
58	6	0	8.277109	-1.423945	1.215379
59	1	0	9.987525	-0.253433	-0.255669
60	1	0	8.888407	0.093192	-1.597748
61	1	0	9.144154	1.300795	-0.319679

62	1	0	9.347775	-1.626597	1.192844
63	1	0	8.009537	-1.134738	2.240008
64	1	0	7.752038	-2.357742	0.976708
65	6	0	2.634896	1.420205	-0.441191
66	1	0	2.513726	2.236474	-1.168304
67	7	0	1.616243	0.908235	0.163444

Rotational constants (GHZ): 0.0675662 0.0581953 0.0316421

DFT of compound PTZPBI.

Standard orientation:

Center Number	Atomic Number	Atomic Type	Coordinates (Angstroms) X	Y	Z

1	6	0	-2.137268	0.382730	0.280341
2	6	0	-3.047734	-0.418217	-0.428822
3	6	0	-4.001980	1.573876	1.257971
4	6	0	-4.426701	-0.200236	-0.351672
5	1	0	-2.648178	-1.220062	-1.035528
6	6	0	-4.897747	0.820084	0.502821
7	1	0	-4.385182	2.328984	1.936839

8	7	0	-5.344292	-0.958245	-1.111299
9	16	0	-6.634189	1.196632	0.541366
10	6	0	-6.571573	-1.350152	-0.525168
11	6	0	-4.831654	-1.744535	-2.223574
12	6	0	-7.269069	-0.453297	0.307414
13	6	0	-7.130103	-2.617274	-0.750126
14	1	0	-4.347273	-2.683270	-1.915980
15	1	0	-5.656677	-1.984004	-2.897027
16	6	0	-8.360297	-2.964634	-0.189099
17	1	0	-6.604402	-3.341300	-1.361058
18	6	0	-9.039522	-2.071691	0.635590
19	1	0	-8.775363	-3.947367	-0.391152
20	1	0	-9.991738	-2.342749	1.079898
21	1	0	-4.104663	-1.145848	-2.775797
22	6	0	-8.478674	-0.820073	0.895156
23	1	0	-8.985758	-0.113474	1.545140
24	6	0	-0.685467	0.080609	0.159343
25	7	0	-0.374937	-1.208437	0.127783
26	6	0	0.319487	1.116133	0.076517
27	6	0	0.926795	-1.594465	0.087708

28	6	0	1.680934	0.715059	0.068632
29	6	0	0.027358	2.506651	-0.044889
30	6	0	1.994069	-0.665939	0.088518
31	6	0	1.224078	-2.991427	0.075505
32	6	0	2.739283	1.673358	0.023391
33	6	0	1.031850	3.442232	-0.090560
34	1	0	-0.994730	2.855674	-0.115889
35	6	0	3.349490	-1.103657	0.085310
36	6	0	2.523799	-3.429499	0.078666
37	1	0	0.408267	-3.705119	0.073964
38	6	0	4.107948	1.265408	0.037243
39	6	0	2.405446	3.052104	-0.041184
40	6	0	0.675207	4.880181	-0.199882
41	6	0	4.423769	-0.166605	0.073504
42	6	0	3.613579	-2.499903	0.087743
43	6	0	2.800394	-4.890599	0.074495
44	6	0	5.091864	2.266207	0.004576
45	6	0	3.423677	4.020429	-0.082153
46	7	0	1.734431	5.797455	-0.226028
47	8	0	-0.481391	5.274047	-0.258211

48	6	0	5.734686	-0.668618	0.082488
49	6	0	4.941691	-2.957885	0.094121
50	7	0	4.145843	-5.283327	0.089495
51	8	0	1.914348	-5.732675	0.059334
52	6	0	4.757346	3.617243	-0.053261
53	1	0	6.141424	1.997384	0.018681
54	6	0	3.098327	5.464854	-0.166667
55	6	0	1.361918	7.213804	-0.323591
56	6	0	5.989736	-2.038210	0.095274
57	1	0	6.578789	0.010916	0.076570
58	6	0	5.246657	-4.410692	0.098383
59	6	0	4.397471	-6.729383	0.091224
60	1	0	5.526696	4.380884	-0.083444
61	8	0	3.965752	6.327232	-0.189556
62	1	0	2.278799	7.797093	-0.338380
63	1	0	0.783365	7.380746	-1.234282
64	1	0	0.741860	7.492511	0.530847
65	1	0	7.006061	-2.415948	0.101919
66	8	0	6.394293	-4.833796	0.108381
67	1	0	3.920366	-7.184990	0.961055

68	1	0	3.971285	-7.180297	-0.807366
69	1	0	5.473574	-6.878217	0.120663
70	6	0	-2.627368	1.375646	1.138858
71	1	0	-1.951058	1.964054	1.748376

Rotational constants (GHZ): 0.0664057 0.0379557 0.0246176

DFT of compound CBZPBI.

Standard orientation:

Center Number	Atomic Number	Atomic Type	Coordinates (Angstroms) X	Y	Z
1	6	0	-2.417107	-0.480690	-0.321729
2	6	0	-3.122544	0.370898	-1.203807
3	6	0	-3.103648	-1.465744	0.401574
4	6	0	-4.500812	0.268632	-1.354105
5	6	0	-4.485049	-1.559105	0.250668
6	1	0	-2.546553	-2.126494	1.055126
7	6	0	-5.202991	-0.689342	-0.616696
8	1	0	-5.021864	0.925466	-2.044094

9	7	0	-5.378382	-2.436627	0.852293
10	6	0	-6.661666	-2.134434	0.412678
11	6	0	-5.042220	-3.450794	1.828808
12	6	0	-6.596802	-1.057750	-0.512574
13	6	0	-7.879284	-2.729014	0.757817
14	1	0	-5.125897	-3.079039	2.857743
15	1	0	-5.707170	-4.309822	1.710559
16	6	0	-9.033886	-2.237386	0.153344
17	1	0	-7.932579	-3.541214	1.475425
18	6	0	-8.986228	-1.177344	-0.769012
19	1	0	-9.992217	-2.682075	0.404882
20	1	0	-9.906294	-0.818442	-1.219407
21	1	0	-4.019900	-3.795451	1.661663
22	1	0	-2.577051	1.091270	-1.803077
23	6	0	-7.773439	-0.583802	-1.104573
24	1	0	-7.739657	0.238348	-1.813641
25	6	0	-0.937940	-0.410893	-0.184839
26	7	0	-0.314101	-1.581574	-0.150994
27	6	0	-0.223497	0.842475	-0.086691
28	6	0	1.042139	-1.628863	-0.095640

29	6	0	1.194717	0.795153	-0.064425
30	6	0	-0.855981	2.114378	0.038091
31	6	0	1.843764	-0.463283	-0.083902
32	6	0	1.679740	-2.906976	-0.082322
33	6	0	1.979103	1.987503	-0.004324
34	6	0	-0.118263	3.271495	0.100247
35	1	0	-1.933992	2.194209	0.096399
36	6	0	3.265492	-0.547963	-0.067468
37	6	0	3.047695	-3.006234	-0.073034
38	1	0	1.068504	-3.802070	-0.090492
39	6	0	3.406476	1.935194	-0.005964
40	6	0	1.309868	3.238179	0.062928
41	6	0	-0.824072	4.573296	0.213935
42	6	0	4.071071	0.627962	-0.043001
43	6	0	3.870515	-1.833753	-0.069663
44	6	0	3.680650	-4.351578	-0.069169
45	6	0	4.108282	3.150232	0.039530
46	6	0	2.053174	4.430157	0.117722
47	7	0	-0.027997	5.726544	0.252339
48	8	0	-2.042711	4.665981	0.265539

49	6	0	5.465998	0.469808	-0.040021
50	6	0	5.270958	-1.944952	-0.063639
51	7	0	5.081837	-4.395342	-0.070938
52	8	0	3.033518	-5.388811	-0.065199
53	6	0	3.445498	4.373937	0.099405
54	1	0	5.191763	3.152649	0.034416
55	6	0	1.375986	5.746548	0.205020
56	6	0	-0.744142	7.003751	0.351240
57	6	0	6.055629	-0.792365	-0.052897
58	1	0	6.113305	1.338738	-0.024416
59	6	0	5.929600	-3.275163	-0.067557
60	6	0	5.686967	-5.732497	-0.072915
61	1	0	3.998368	5.305949	0.139808
62	8	0	1.999547	6.798718	0.240084
63	1	0	-0.003514	7.799087	0.357554
64	1	0	-1.421235	7.113525	-0.498147
65	1	0	-1.338954	7.024239	1.266713
66	1	0	7.134114	-0.904093	-0.050242
67	8	0	7.146729	-3.398060	-0.067144
68	1	0	5.369724	-6.283240	0.814945

69	1	0	5.355930	-6.285736	-0.954032
70	1	0	6.766495	-5.607480	-0.081062

Rotational constants (GHZ): 0.0727574 0.0417808 0.0270324

DFT of compound NNDPBI.

Standard orientation:

Center Number	Atomic Number	Atomic Type	Coordinates (Angstroms) X	Y	Z

1	6	0	5.300259	1.160955	0.216808
2	6	0	4.248295	2.073766	0.230294
3	6	0	2.910836	1.653439	0.151096
4	6	0	2.653980	0.253741	0.064520
5	6	0	3.730455	-0.673778	0.040297
6	6	0	5.053501	-0.208248	0.118375
7	6	0	1.322000	-0.244718	-0.007829
8	6	0	1.063624	-1.632892	-0.106552
9	6	0	2.168230	-2.538996	-0.144902

10	6	0	3.456981	-2.075900	-0.070077
11	6	0	1.773336	2.579269	0.133643
12	6	0	0.450016	2.050286	0.035621
13	6	0	0.217743	0.641250	-0.011042
14	6	0	1.920095	3.974414	0.195893
15	6	0	0.819880	4.826892	0.145912
16	6	0	-0.472196	4.317256	0.029533
17	6	0	-0.666847	2.925730	-0.022687
18	6	0	-1.980098	2.381548	-0.164353
19	6	0	-2.182764	1.022746	-0.204994
20	6	0	-1.096306	0.109219	-0.082311
21	6	0	4.582934	-3.045923	-0.101717
22	7	0	5.879352	-2.518687	-0.014816
23	6	0	6.196391	-1.154611	0.094715
24	6	0	-1.621719	5.249474	-0.049541
25	7	0	-2.891091	4.666437	-0.204955
26	6	0	-3.148053	3.290070	-0.276384
27	8	0	4.417120	-4.253389	-0.198225
28	8	0	7.357420	-0.775043	0.165396
29	8	0	-1.482663	6.463935	0.010191

30	8	0	-4.295093	2.886241	-0.415117
31	6	0	6.976469	-3.492809	-0.045403
32	6	0	-4.059575	5.548486	-0.302529
33	1	0	6.329906	1.495375	0.276606
34	1	0	4.484715	3.129056	0.299730
35	1	0	1.975022	-3.602705	-0.222940
36	1	0	2.907104	4.413727	0.278441
37	1	0	0.946392	5.903094	0.188335
38	1	0	-3.194504	0.665861	-0.347506
39	1	0	6.874258	-4.190663	0.788138
40	1	0	6.937405	-4.063949	-0.975159
41	1	0	7.910500	-2.942048	0.027753
42	1	0	-4.563820	5.390095	-1.258074
43	1	0	-4.765060	5.316244	0.497756
44	1	0	-3.708322	6.573636	-0.219734
45	7	0	-0.192639	-2.142705	-0.128669
46	6	0	-1.244999	-1.331447	-0.076333
47	6	0	-2.561542	-2.001293	-0.017434
48	6	0	-3.621165	-1.552189	0.789767
49	6	0	-2.761674	-3.198133	-0.728926

50	6	0	-4.827386	-2.235096	0.859428
51	1	0	-3.493070	-0.675249	1.415955
52	6	0	-3.964111	-3.882995	-0.683401
53	1	0	-1.946281	-3.586814	-1.329198
54	6	0	-5.044111	-3.412430	0.104783
55	1	0	-5.598639	-1.855467	1.517280
56	1	0	-4.066026	-4.791761	-1.263063
57	7	0	-6.252823	-4.077422	0.138288
58	6	0	-6.396082	-5.358533	-0.533604
59	6	0	-7.307059	-3.623058	1.029624
60	1	0	-7.419517	-5.714208	-0.411069
61	1	0	-6.202019	-5.268846	-1.609240
62	1	0	-5.717839	-6.123638	-0.129010
63	1	0	-8.196309	-4.234454	0.873236
64	1	0	-7.024536	-3.696161	2.090240
65	1	0	-7.579274	-2.581384	0.822887

Rotational constants (GHZ): 0.0878413 0.0563605 0.0346915

References

[1]. De, Joydip, et al. "High hole mobility and efficient ambipolar charge transport in heterocoronene-based ordered columnar discotics." *Journal of the American Chemical Society* 141.47 (2019): 18799-18805.

[2]. Tiwari, Nikhil Ji, et al. "Charge Carrier Mobility of Phenothiazine Functionalized TCBD Derivatives of Naphthalimide." *Chemistry–An Asian Journal*: e00259.

[3]. Yadav, Kajal, et al. "Columnar self-assembled heteroatom bay-annulated perylene bisimide as passivating layer for high performance perovskite solar cells." *Solar Energy* 278 (2024): 112762.

[4]. Frisch, M. J.; Trucks, G. W.; Schlegel, G. W.; Scuseria, G. E.; Robb, M. A.; Cheeseman, J. R.; Scalmani, G.; Barone, V.; Petersson, G. A.; Li, Nakatsuji, X.; Caricato, M.; Marenich, A.; Bloino, J.; Janesko, B. G.; Gomperts, R.; Mennucci, B.; Hratchian, H. P.; Ortiz, J. V.; Izmaylov, A. F.; Sonnenberg, J. L.; Williams-Young, D.; Ding, F.; Lipparini, F.; Egidi, F.; Goings, J.; Peng, B.; Petrone, A.; Henderson, T.; Ranasinghe, D.; Zakrzewski, V. G.; Gao, J.; Rega, N.; Zheng, G.; Liang, W.; Hada, M.; Ehara, M.; Toyota, K.; Fukuda, R.; Hasegawa, J.; Ishida, M.; Nakajima, T.; Honda, Y.; Kitao, O.; Nakai, H.; Vreven, T.; Throssell, K.; Montgomery, J. A.; Peralta, J. E., Jr.; Ogliaro, F.; Bearpark, M.; Heyd, J. J.; Brothers, E.; Kudin, K. N.; Staroverov, V. N.; Keith, T.; Kobayashi, R.; Normand, J.; Raghavachari, K.; Rendell, A.; Burant, J. C.; Iyengar, S. S.; Tomasi, J.; Cossi, M.; Millam, J. M.; Klene, M.; Adamo, C.; Cammi, R.; Ochterski, J. W.; Martin, R. L.; Morokuma, K.; Farkas, O.; Foresman, J. B.; Fox, D. J. Gaussian 09, rev. A.02; Gaussian, Inc.: Wallingford, CT, **2016**.